

## V. THEORETICAL PHYSICS

### OVERVIEW

Theoretical research in the Physics Division addresses a broad range of problems involving the structure and dynamics of hadrons and nuclei. There is a strong emphasis on comparison to data from Argonne's ATLAS facility, TJNAF, and other laboratories around the world. Our work includes the modeling and application of quantum chromodynamics to light- and heavy-hadron structure at zero temperature and density, and at the extremes of temperature and density appropriate to the early universe, neutron stars, and upcoming RHIC and LHC experiments. We develop reaction theories for meson and nucleon-resonance production experiments at JLab, and for medium effects on mesons and resonances in nuclei and dense matter relevant to RHIC. We construct realistic two- and three-nucleon potentials that give accurate fits to NN elastic scattering data and trinucleon properties, and use them in detailed many-body calculations of light nuclei, closed-shell nuclei, nuclear matter and neutron stars, and in a variety of astrophysically important electroweak reactions. Our nuclear structure and reaction studies include coupled-channels calculations of heavy-ion reactions near the Coulomb barrier, and calculations of observables in breakup reactions of nuclei far from stability. We also study high-spin superdeformation, spectroscopy of the heaviest elements ( $A \geq 250$ ), and nuclear structure near the proton-drip line. Additional research is made in atomic physics, neutron physics, quantum computing and fundamental quantum mechanics. Several of our projects involve major numerical simulations using the massively parallel computer systems at Argonne and NERSC.

## A. NUCLEAR DYNAMICS WITH SUBNUCLEONIC DEGREES OF FREEDOM

The objective of this research program is to investigate the role of quark-gluon degrees of freedom in hadrons, and the role of mesons and nucleon resonance degrees of freedom in nuclei.

At the level of quark-gluon degrees of freedom, the Dyson-Schwinger equations (DSEs) provide a Poincaré covariant, nonperturbative method for studying QCD in the continuum. The existence of symmetry preserving truncations makes possible the exploration of phenomena such as: confinement, dynamical chiral symmetry breaking, and bound state structure and interactions. In addition, they provide a generating tool for perturbation theory and hence yield model-independent results for the ultraviolet behavior of strong interaction observables. This means that model applications link physical processes to the long-range interaction in QCD, which is poorly understood and whose elucidation is a key goal of contemporary experimental programs. The last year has seen many successful applications. For example, we calculated the valence-quark momentum-distribution in the pion and demonstrated that quark confinement, as exhibited in the momentum-space extent of the pion's Bethe-Salpeter amplitude, is observable in the large- $x$  behavior of the distribution. We found that the related phenomenon of dynamical chiral symmetry breaking magnifies, by a factor of at least 40, the contribution from current-quark electric dipole moments (EDMs) to the neutron's EDM, which makes this observable an even more severe constraint on extensions of the standard model. We explored the embedding of aspects of QCD in a quantum Vlasov equation and showed that plasma oscillations in the pre-equilibrium stage of quark gluon plasma formation can signal their presence via observable effects on the thermal dilepton spectrum.

At the level of mesons and nucleon resonance degrees of freedom, a dynamical approach was developed to describe  $\pi N$  and  $\gamma N$  reactions, and used to explore the structure of nucleon resonances using the recent data from TJNAF, MIT-Bates, LEGS, and other electron facilities around the world. From the investigation of pion production, it was found that the deformation of the  $\Delta$  is mainly due to the pion cloud and the extracted  $\gamma N \rightarrow \Delta$  form factors are consistent with the predictions from constituent quark models. In the investigation of the production of vector mesons and kaons, the importance of coupled-channel effects was demonstrated and some higher mass nucleon resonances were identified. Efforts were made to resolve some long-standing problems in pion-nucleus scattering by using the nuclear wave functions from quantum Monte Carlo calculations at Argonne. We also continued our investigation of compressed strange matter and have started an investigation of  $J/\Psi$  propagation in the pion system, aimed at addressing some questions related to the data from RHIC.

### a.1. $K \rightarrow \pi\pi$ and a Light Scalar Meson (J. C. R. Bloch, C. D. Roberts, S. M. Schmidt, M. A. Ivanov,\* and T. Mizutani†)

We explored the  $\Delta I = 1/2$  rule and the fundamental CP violating gauge:  $\epsilon'/\epsilon$  in  $K \rightarrow \pi\pi$  transitions using the Dyson-Schwinger equations. Exploiting the feature that QCD penguin operators direct  $K_S^0$  transitions through  $0^{++}$  intermediate states, we find an explanation of the enhancement of  $I = 0$   $K \rightarrow \pi\pi$  transitions in the contribution of a light  $\sigma$ -meson,  $m_\sigma \approx 0.5$  GeV. This

mechanism also affects  $\epsilon'/\epsilon$  providing a significant enhancement. The study shows that the effect of this  $\sigma$ -meson should be understood before any conclusions can be drawn about non-Standard-Model effects in parity violating K-decays. An article describing this work has been published.<sup>1</sup>

\*BLTP, JINR, Dubna, Russia; †Virginia Polytechnic Institute and State University, Blacksburg, VA

<sup>1</sup>J. C. R. Bloch, C. D. Roberts, S. M. Schmidt, M. A. Ivanov, and T. Mizutani, Phys. Rev. C 62, 025206 (2000).

### a.2. Selected Nucleon Form Factors and a Composite Scalar Diquark

(J. C. R. Bloch, C. D. Roberts, and S. M. Schmidt)

As an application and test of our quark-plus-scalar-diquark nucleon model, we calculated a wide range of leptonic and nonleptonic nucleon form factors: pseudoscalar, isoscalar- and isovector-vector, axial-vector and scalar. The last yields the nucleon  $\sigma$ -term and on-shell  $\sigma$ -nucleon coupling. The calculated form factors are soft and there is no sign that this is a model-dependent result; the couplings are generally in good agreement with experiment and other determinations. Elements in the dressed-quark-axial-vector vertex that

are not constrained by the Ward-Takahashi identity contribute  $\sim 20\%$  to the magnitude of  $g_A$ . We anticipate a contribution of similar magnitude from the axial-vector diquark correlation, hitherto omitted. The calculation of the nucleon  $\sigma$ -term is particularly interesting because it illustrates the only method that allows an unambiguous off-shell extrapolation in the estimation of meson-nucleon form factors. An article describing this work has been published.<sup>1</sup>

<sup>1</sup>J. C. R. Bloch, C. D. Roberts, and S. M. Schmidt, Phys. Rev. C **61**, 065207 (2000).

### a.3. Temperature-Dependence of Pseudoscalar and Scalar Correlations

(C. D. Roberts, S. M. Schmidt, P. Maris,\* and P. C. Tandy\*)

In order to elucidate hadronic signals of quark-gluon plasma formation we solved the inhomogeneous pseudoscalar and scalar Bethe-Salpeter equations using a renormalization-group-improved rainbow-ladder truncation. The solutions exhibit bound state poles below and above  $T_c$ , the critical temperature for chiral symmetry restoration, *i.e.*, the bound states persist into the quark-gluon plasma. Above  $T_c$  the bound state amplitudes are identical, as are the positions and residues of the pseudoscalar and scalar poles in the vertices, so these composites are identical in the

absence of dynamical chiral symmetry breaking. We found that in the chiral limit the  $\pi^0 \rightarrow \gamma\gamma$  coupling vanishes at  $T_c$ , as do  $f_\pi$ ,  $m_\sigma$  and  $g_{\sigma\pi\pi}$ . Furthermore, for light current-quark masses the  $2\pi$  decay channel of the isoscalar-scalar meson remains open until very near  $T_c$ , and the widths of the dominant pion decay modes remain significant in the vicinity of the crossover. Therefore one cannot expect to identify the quark-gluon plasma via a marked increase in the  $\sigma$ -meson lifetime. An article describing this research has been published.<sup>1</sup>

\*Kent State University

<sup>1</sup>C. D. Roberts, S. M. Schmidt, P. Maris, and P. C. Tandy, Phys. Rev. C **63**, 025202 (2001).

### a.4. Temperature, Chemical Potential and the $\rho$ -Meson (C. D. Roberts and S. M. Schmidt)

Nonperturbative Dyson-Schwinger equation (DSE) studies provide a means of exploring deconfinement, chiral-symmetry restoration, and hadron properties at nonzero temperature,  $T$ , and chemical potential,  $\mu$ . Using a simple DSE-model we found that there is a line in the  $(\mu, T)$ -plane along which the  $\rho$ -meson mass retains its vacuum value. This feature is tied to a long-standing DSE prediction that the dressed-quark mass-

function is strongly momentum-dependent in the infrared domain; *i.e.*, momenta less than 1 GeV. We proposed that this momentum-dependence should be incorporated in quantum Vlasov equation studies of quark-gluon plasma formation and equilibration, and indicated how that might proceed. An article describing this work has been published.<sup>1</sup>

<sup>1</sup>C. D. Roberts and S. M. Schmidt, Proc. of the International Workshop XXVIII on Gross Properties of Nuclei and Nuclear Excitations, edited by M. Buballa, W. Nörenberg, B.-J. Schaefer and J. Wambach (GSI mbH, Darmstadt 2000), pp. 185-191.

### a.5. Dyson-Schwinger Equations: Density, Temperature and Continuum Strong QCD (C. D. Roberts and S. M. Schmidt)

Continuum strong QCD is the application of models and continuum quantum field theory to the study of phenomena in hadronic physics, which includes; *e.g.*, the spectrum of QCD bound states and their interactions, and the transition to, and properties of, a quark-gluon plasma. We prepared a review article that provides a contemporary perspective, couched primarily in terms of the Dyson-Schwinger equations but also making comparisons with other approaches and models. Our discourse provided a practitioners' guide to features of the Dyson-Schwinger equations (such as confinement and dynamical chiral symmetry breaking) and canvassed phenomenological applications to light meson and baryon properties in cold, sparse QCD. This provided the foundation for an extension of our review

to hot, dense QCD, which is probed via the introduction of the intensive thermodynamic variables: chemical potential and temperature. We described order parameters whose evolution signals deconfinement and chiral-symmetry restoration, and chronicled their use in demarcating the quark-gluon plasma phase boundary and characterizing the plasma's properties. Hadron traits change in an equilibrated plasma. We exemplified this and discussed putative signals of the effects. Finally, since plasma formation is not an equilibrium process, we discussed recent developments in kinetic theory and its application to describing the evolution from a relativistic heavy-ion collision to an equilibrated quark gluon plasma. Our review has been published.<sup>1</sup>

<sup>1</sup>C. D. Roberts and S. M. Schmidt, Prog. Part. Nucl. Phys. **45**, S1-S103 (2000).

### a.6. Valence-Quark Distributions in the Pion (M. B. Hecht, C. D. Roberts, and S. M. Schmidt)

The cross section for deep inelastic lepton-hadron scattering can be interpreted in terms of the momentum-fraction probability distributions of quarks and gluons in the hadronic target, and since the pion is a two-body bound state with only *u*- and *d*-valence-quarks it is, in some respects, the simplest hadron and therefore represents the least complicated, nontrivial system for which these distribution functions can be calculated. The DSEs provide an approach well-suited to the study of pion observables because a chiral symmetry preserving truncation scheme exists and therefore they easily capture the dichotomous bound-state/Goldstone-mode character of the pion. We calculated the pion's valence-quark momentum-fraction probability distribution using a Dyson-Schwinger equation model and found that valence-quarks with an active mass of

0.30 GeV carry 71% of the pion's momentum at a resolving scale  $q_0=0.54$  GeV= $1/(0.37$  fm). The shape of our calculated distribution is characteristic of a strongly bound system and, evolved from  $q_0$  to  $q=2$  GeV, it yields first, second and third moments in agreement with lattice and phenomenological estimates, and valence-quarks carrying 49% of the pion's momentum. Nevertheless, there is a pointwise difference between our calculated distribution and the form used hitherto in parametrizing pion data but, from the information currently available, its origin does not appear to lie in model details. Indeed, it may be attributable to the restricted function space used thus far in parametrizing pion data. An article describing this work has been published.<sup>1</sup>

<sup>1</sup>M. B. Hecht, C. D. Roberts, and S. M. Schmidt, Phys. Rev. C **63**, 025213 (2001).

### a.7. Contemporary Applications of Dyson-Schwinger Equations (M. B. Hecht, C. D. Roberts and S. M. Schmidt)

The contemporary application of DSEs is well illustrated by the calculation of pseudoscalar meson masses and the study of nucleon observables. For the former, we showed that a direct solution of the appropriate Bethe-Salpeter equations, combined with the knowledge provided by a DSE-derived model-independent mass-formula, predicts the current-quark-mass-dependence of pseudoscalar meson masses recently measured in lattice-QCD simulations. Importantly our analysis also provides an intuitive understanding, relating the evolution to a large value of

the vacuum and in-hadron quark condensates. For the latter, we showed that a Poincaré covariant Fadde'ev equation, which describes a baryon as a composite of a dressed quark and nonpointlike, dressed scalar and axial-vector diquarks, provides an internally consistent picture of the nucleon and  $\Delta$ . Furthermore, our preliminary study indicated that the  $\pi$ -loop correction to the calculated nucleon mass is small. This, perhaps surprising, result is the subject of ongoing research. An article describing this has been submitted for publication.<sup>1</sup>

<sup>1</sup>M. B. Hecht, C. D. Roberts, and S. M. Schmidt, submitted to the Proceedings of the 4th International Conference on Quark Confinement and the Hadron Spectrum, 3-8 July 2000, Vienna, Austria.

### a.8. Diquarks and Density (M. B. Hecht, C. D. Roberts, and S. M. Schmidt)

A diquark is a bosonic quark-quark correlation, which is necessarily colored in all but 2-color QCD (QC<sub>2</sub>D). Therefore, in the presence of color-confinement, diquarks cannot be directly observed in an  $N_c \geq 3$  color gauge theory's spectrum. Nevertheless, evidence is accumulating, *e.g.*, via Fadde'ev equation studies, which suggests that confined diquark correlations play an important role in hadronic spectroscopy and interactions. The significance of diquarks in those applications motivates a study of the possibility that dense hadronic matter may exhibit diquark condensation, *i.e.*, quark-quark pairing promoted by a quark chemical potential. To explore this we introduced a Gorkov-Nambu-like gap equation for QCD and applied it to QC<sub>2</sub>D and, in two qualitatively

different truncations, to QCD itself. Among other interesting features, we demonstrated that QC<sub>2</sub>D with massive fermions undergoes a second-order transition to a superfluid phase when the chemical potential exceeds  $m_\pi/2$ . In the QCD application we illustrated that the  $\sigma: = -\langle \bar{q}q \rangle^{1/3} \neq 0$  phase, which determines the properties of the strong-interaction's mass spectrum at zero temperature and chemical potential, is unstable with respect to the superfluid phase when the chemical potential exceeds  $\approx 2\sigma$ , and that at this point the diquark gap is large,  $\approx \sigma/2$ . This superfluid phase survives to temperatures greater than that expected in the core of compact stars. An article describing this work has been submitted for publication.<sup>1</sup>

<sup>1</sup>M. B. Hecht, C. D. Roberts, and S. M. Schmidt, submitted to the Proceedings of Physics of Neutron Star Interiors, ECT\*, Trento, Italy, June-July 2000, eds. D. Blaschke, N. K. Glendenning and A. Sedrakian.

**a.9. Pair Creation and Plasma Oscillations** (M. B. Hecht, C. D. Roberts, S. M. Schmidt, A. V. Prozorkevich,\* and D. V. Vinnik\*)

Ultra-relativistic heavy-ion collisions (URHICs) are very complicated processes and their understanding requires a microscopic modeling of all stages: the formation, evolution and hadronization of a strongly-coupled plasma. With RHIC now operating it is imperative to develop a microscopic understanding of URHICs, including their non-equilibrium aspects. In response to this challenge we studied particle creation in strong fields in the presence of thermalizing collisions. Our quantum kinetic equation involved a non-Markovian source term and a relaxation time approximation to the collision term, and the strong electric background field was determined by coupling-

in Maxwell's equation and solving the whole system self-consistently. Plasma oscillations are an almost inevitable outcome of this treatment. We found that the plasma frequency depends on at least three quantities: the field strength, the relaxation time and the mass distribution of the produced particles. In addition, we observed that incorporating a strongly momentum-dependent dressed-parton mass, which is an essential feature of QCD, can have a significant impact on the evolution of the plasma. In particular it promotes plasma oscillations. An article describing this work has been submitted for publication.<sup>1</sup>

\*Saratov State University, Armenia

<sup>1</sup>A. V. Prozorkevich, D. V. Vinnik, S. M. Schmidt, M. B. Hecht and C. D. Roberts, submitted to the Proceedings of Quark Matter in Astro- and Particlephysics, University of Rostock, Germany, 27-29 November 2000, eds. D. Blaschke, G. Baur and S. M. Schmidt

**a.10. Neutron Electric Dipole Moment: Constituent-Dressing and Compositeness** (M. B. Hecht, C. D. Roberts, and S. M. Schmidt)

The action for any local quantum field theory is invariant under the transformation generated by the anti-unitary operator CPT, which is the product of the inversions: C, charge conjugation, P, parity transformation, and T, time reversal. The decay of the CP-odd eigenstate  $K_L^0$  into a CP-even  $2\pi$  final state demonstrates that the product of only C and P is not a good symmetry of the standard model. This entails that time reversal invariance must also be violated and that too has been observed in detailed studies of the neutral kaon system. It has long been known that the possession of an electric dipole moment (EDM) by a spin-1/2 particle would signal the violation of time-reversal invariance. (The existence of a dipole moment signals a spherically asymmetric distribution of charge.) Any such effect is likely small, given the observed magnitude of CP and T violation in the neutral kaon system, and this makes neutral particles the obvious subject for experiments, the existence of an electric monopole charge would overwhelm most signals of the dipole strength. It is therefore natural to focus on the

neutron, which is the simplest spin-1/2 neutral system in nature. Attempts to measure the neutron's EDM,  $d_n$ , have a long history and currently yield the upper bound:  $|d_n| < 6.3 \times 10^{-26} e \text{ cm}$  (90% C.L.). This has proven to be an effective constraint on attempts to extend the standard model and to assist in this we have calculated  $d_n$  using a well-constrained *Ansatz* for the nucleon's Poincaré covariant Fadde'ev amplitude. We found that the momentum-dependent quark dressing amplifies the contribution from the current-quarks' EDMs, and that dressed-quark confinement and binding make distinguishable the effect of the two CP and T violating interactions:  $i\gamma_5\sigma_{\mu\nu}(p_1 - p_2)^0$  and  $\gamma_5(p_1 + p_2)_\mu$ , where  $p_1$  and  $p_2$  are the current-quarks' momenta. In addition, our calculation showed that the value of  $|d_n|$  obtained using the current-quark EDMs generated by a minimal three Higgs doublet model of spontaneous CP violation is perilously close to the experimental upper bound, *i.e.*, that the so-called Weinberg model is almost excluded by this bound. An article describing our work has been submitted for publication.

**a.11. Plasma Production and Thermalization in a Strong Field** (M. B. Hecht, C. D. Roberts, S. M. Schmidt, D. V. Vinnik,\* A. V. Prozorkevich,† S. A. Smolyansky,‡ and V. Toneev‡)

We have extended and improved the collision term in our quantum Vlasov equation, and reanalyzed aspects of the formation and equilibration of a quark-gluon plasma (QGP). In addition, since leptons do not participate in the strong interactions that equilibrate the QGP, we calculated the thermal dilepton spectrum produced by the evolving plasma. We again found that field-current feedback generates plasma oscillations in all thermodynamic observables. The oscillations were also evident in the production rate of thermal dileptons.

While the time evolution of that rate may not be measurable, the plasma oscillations also acted to significantly enhance the time integrated rate, which is easily accessible. This effect was marked by a sharp increase in the dilepton yield once the energy-density per parton became large enough to generate a high-frequency and large-amplitude plasma oscillation, which could survive the effect of damping for a significant time after the moment of impact. An article describing this work has been submitted for publication.

\*University of Rostock, Germany †Saratov State University, Armenia; ‡BLTP, JINR, Dubna, Russia

**a.12. Axial-Vector Diquarks in the Baryon** (M. B. Hecht, C. D. Roberts and S. M. Schmidt)

We have shown that a product *Ansatz* for the nucleon's Fadde'ev amplitude using only a scalar- diquark provides a good description of leptonic and nonleptonic couplings and form factors, with some notable exceptions, *e.g.*,  $\langle r_{\text{fl}}^2 \rangle$ ,  $g_A$ . Properly incorporating the lower component of the nucleon's spinor helps somewhat in addressing these exceptions. However, discrepancies remain and we anticipate that their amelioration requires the inclusion of axial-vector

diquark correlations. Furthermore, without axial-vector diquark correlations one cannot describe the  $\Delta$  resonance, and the  $N \rightarrow \Delta$  transition is an important probe of hadron structure and models, *e.g.*, resonant quadrupole strength in this transition can be interpreted as a signal of nucleon deformation. Hence we are working on improving the *Ansatz* by including these qualitatively important correlations.

**a.13. J/Ψ Suppression as a Signal of Quark Gluon Plasma Formation** (M. B. Hecht, C. D. Roberts, S. M. Schmidt, and D. B. Blaschke\*)

We have developed a successful approach to describing heavy-meson observables at zero temperature. That makes possible a reliable extrapolation into the domain of nonzero temperature, which is relevant to the program at RHIC. The suppression of the J/Ψ production cross section has been touted as a unique signal for quark-gluon plasma formation, and such a suppression has been observed at CERN. We propose to study J/Ψ production in the expectation that additional insight will follow from the Dyson-Schwinger equations' capacity to unify nonperturbative aspects of light- and heavy-meson observables via a microscopic description using QCD's elementary

excitations. Our initial focus is the T-dependence of J/Ψ break-up by hadronic co-movers; *i.e.*, the *substructure induced* T-dependence of the interactions with other mesons in the medium that dissociates the J/Ψ. These processes are likely to be affected by the dramatic T-dependence of the dressed-light-quark mass function in the neighborhood of the QGP phase boundary and a possible T-dependent reduction in the mass of the open-charm final states. Our goal is to elucidate the mechanisms involved and the fidelity of J/Ψ suppression as a signal of quark gluon plasma formation.

\*University of Rostock, Germany

**a.14. Valence-Quark Distributions in the Nucleon** (M. B. Hecht, C. D. Roberts, S. M. Schmidt, J. C. R. Bloch\*)

The pion provides the simplest theoretical subject for a calculation of the valence-quark distribution function. However, pion targets are not readily available for experiment and the most reliable measurements of quark distribution functions have been performed on nucleon targets. We are therefore extending the approach we developed for the pion in order to employ it in a calculation of the nucleon's valence-quark distribution. The target nucleon is again represented by our phenomenologically successful scalar-diquark product *Ansatz* for its Fadde'ev amplitude. Our study

will provide the first realistic, Poincaré covariant calculation of this observable. It will make possible the drawing of a connection between deep-inelastic scattering measurements and the “soft physics” wrapped up in nucleon structure. For example, it will provide a means of testing the validity and importance of diquark clustering in the nucleon, and the relation between the d/u-ratio at large- $x$  and confinement, as it is exhibited in the momentum-space extent of the Fadde'ev amplitude.

---

\*University of Tübingen, Germany

**a.15. Dynamical Study of the N\* Excitation in N(e,e'π) Reactions** (T.-S. H. Lee and T. Sato\*)

The dynamical model we developed<sup>1</sup> has been applied to pion electroproduction reactions on the nucleon. It is found that the model can describe, to a very large extent, the recent data on  $p(e,e'\pi^0)$  reactions from Jefferson Lab and MIT-Bates, as shown in Fig. V-1. The magnetic dipole (M1), electric dipole (E2), and Coulomb (C2) strengths of the  $\gamma N \rightarrow \Delta$  transition have been extracted. It is found that the C2/M1 ratio drops significantly with  $Q^2$  and reaches about -14% at  $Q^2 = 4$  (GeV/c)<sup>2</sup>, while the E2/M1 ratio remains close to the value  $\sim -3\%$  at the  $Q^2 = 0$  photon point. The extracted

M1 transition form factor drops faster than the usual dipole form factor of the proton, as shown in Fig. V-2. We also find that the nonresonant interactions can dress the  $\gamma N \rightarrow \Delta$  vertex to significantly enhance its strength at low  $Q^2$ , but much less at high  $Q^2$ . Predictions are presented for future experimental test. A paper describing our results has been submitted for publication. We have now extended the model to investigate N\* excitations in P<sub>11</sub> and S<sub>11</sub> channels. The main task is to include the coupling with  $\pi\pi N$  channels.

---

\*Osaka University, Japan

<sup>1</sup>T. Sato and T.-S. H. Lee, Phys. Rev. C **54**, 2660 (1996).



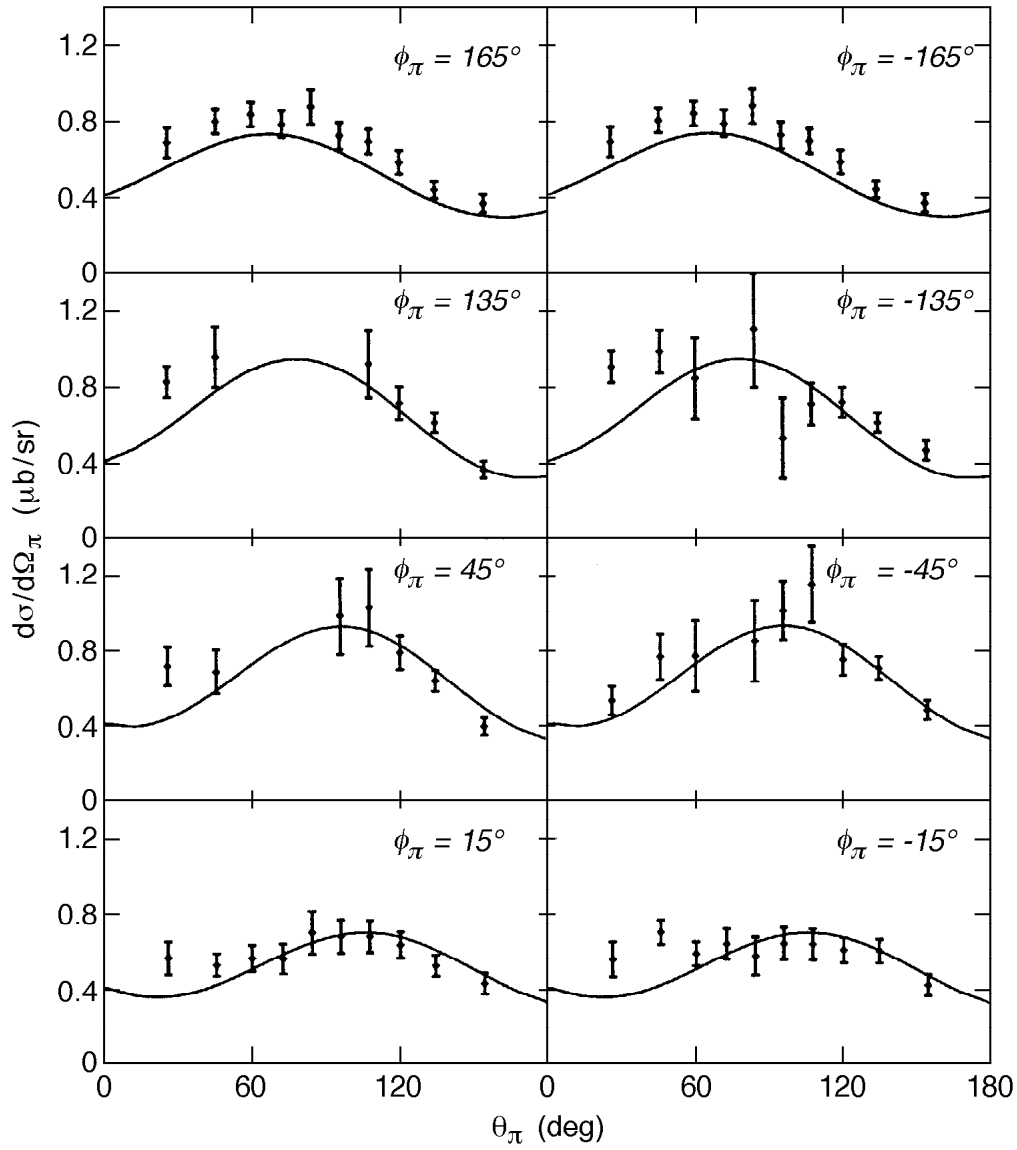


Fig. V-1. The predicted  $p(e, e' \pi^0)$  differential cross sections at invariant mass  $W=1235$  MeV,  $Q^2 = 2.8$  (GeV/c) $^2$  are compared with the JLab data.

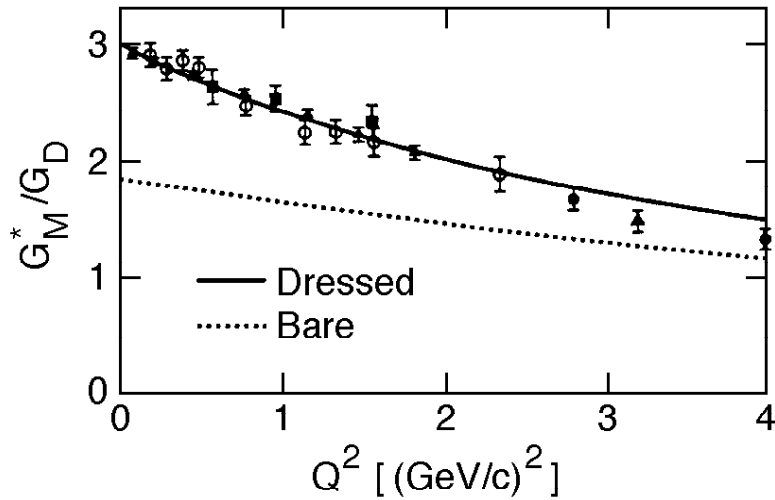


Fig. V-2. The ratio between the M1 form factor of the  $\gamma N \rightarrow \Delta$  transition and the proton dipole form factor  $G_D$ . The solid (dotted) curve is the ratio for the dressed (bare) M1 form factor.

#### a.16. Nucleon Resonances in $\omega$ Photoproduction (T.-S. H. Lee, Yongseok Oh,\* and Alexander I. Titov†)

The role of the nucleon resonances ( $N^*$ ) in  $\omega$  photoproduction is investigated by using the resonance parameters predicted by Capstick and Roberts.<sup>1</sup> In contrast with the previous investigations based on the  $SU(6) \times O(3)$  limit of the constituent quark model, the employed  $N^* \rightarrow \gamma N$  and  $N^* \rightarrow \omega N$  amplitudes include the configuration mixing effects due to the residual quark-quark interactions. The contributions from the nucleon resonances are found to be significant relative to the nonresonant amplitudes in changing the differential cross sections at large scattering angles. This is shown in Fig. V-3. We suggest that a crucial test of our predictions can be made by measuring the parity asymmetry and beam-target double asymmetry at forward scattering angles. The dominant contributions are found to be from  $N1/2^+(1910)$ , a missing resonance, and  $N3/2^-(1960)$  which is identified as the  $D_{13}(2080)$  of the Particle Data Group. Our predictions are illustrated in Fig. V-4. A paper describing our results has been submitted for publication.

\*Academia Sinica, Taiwan; †JINR, Dubna, Russia

<sup>1</sup>S. Capstick and C. D. Roberts, Phys. Rev. D **46**, 2864 (1992); **49**, 4570 (1994).

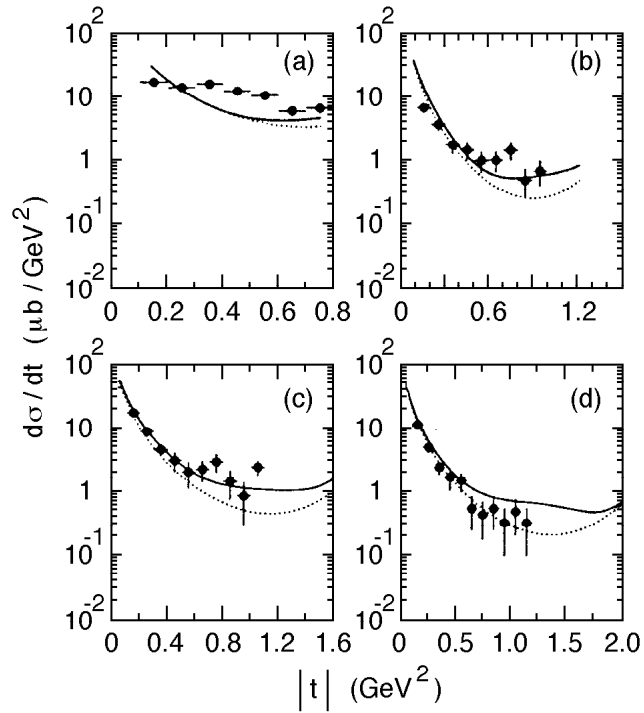


Fig. V-3. Differential cross sections for the  $\gamma p \rightarrow p\omega$  reaction as a function of  $|t|$  at different energies:  $E_\gamma =$  (a) 1.23, (b) 1.45, (c) 1.68, and (d) 1.92 GeV. The solid and dotted curves are calculated respectively with and without including  $N^*$  effects.

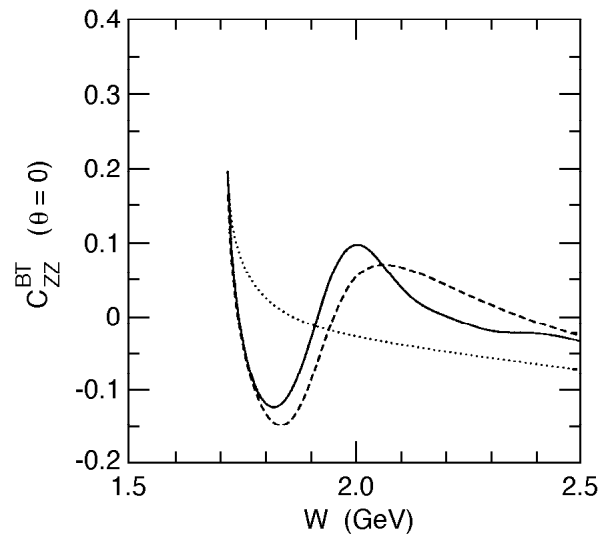


Fig. V-4. Beam-target asymmetry  $C_{ZZ}^{\text{BT}}$  at  $\theta = 0$  as a function of invariant mass  $W$ .

**a.17. Coupled-channel Approach for  $K^+\Lambda$  Photoproduction** (T.-S. H. Lee, Wen-Tai Chiang,\* F. Tabakin,\* and B. Saghai†)

We study kaon photoproduction on nucleons in a coupled-channel (CC) approach. A general method to include multi-step final-state interactions of strangeness electro-magnetic production is developed, and then applied numerically to investigate the  $\gamma p \rightarrow K^+\Lambda$  process. In addition to direct  $K^+\Lambda$  production, we incorporate both  $\pi^0 p$  and  $\pi^+ n$  pion-nucleon channels into our CC approach. Cross sections are calculated

and compared to recent data from SAPHIR, with emphasis on the CC effects. We show that the CC effects due to the  $\pi N$  channels are significant at the level of inducing 20% changes on total cross sections; thereby demonstrating the need to include  $\pi N$  coupled-channels to correctly describe strangeness electromagnetic production. A paper describing our results is being prepared for publication.

\*University of Pittsburgh; †CEA-Saclay, France

**a.18. Meson-exchange  $\pi N$  Models in Three-dimensional Bethe-Salpeter Formulation** (T.-S. H. Lee, Cheng-Tsung Hung,\* and Shin Nan Yang†)

Pion-nucleon scattering is investigated by using several three-dimensional reduction schemes of the Bethe-Salpeter equation for a model Lagrangian involving  $\pi$ ,  $N$ ,  $\Delta$ ,  $\rho$ , and  $\sigma$  fields. It is found that all of the resulting meson-exchange models give similar good descriptions of the  $\pi N$  scattering data up to 400 MeV. However, they have significant differences in describing the  $\pi NN$  and  $\pi N\Delta$  form factors and the  $\pi N$  off-shell t-matrix

elements. We show that these differences can be best distinguished by investigating the near-threshold pion production from nucleon-nucleon collisions and pion photoproduction on the nucleon. The consequences of using these models to investigate various pion-nucleus reactions are also discussed. A paper describing our results has been submitted for publication

\*Chung-Hua Institute of Technology, Taiwan, †National Taiwan University

**a.19.  $\phi$ -N Bound State** (T.-S. H. Lee, H. Gao,\* and V. Marinov\*)

It has been suggested that the QCD van der Waals interaction, mediated by multi-gluon exchange, is dominant when the interacting two-color singlet hadrons have no common quarks. We have found that such a QCD van der Waals force is strong enough to bind a  $\phi$  meson onto a nucleon inside a nucleus to form a bound state. The direct experimental signature for

such an exotic state is proposed in the case of sub-threshold  $\phi$  meson photo-production from nuclear target. Our results for a  $^{12}\text{C}$  target are shown in Fig. V-5. The predicted rates indicate the feasibility of such an experiment at JLab. A paper describing our results has been submitted for publication.

\*MIT, Cambridge, MA

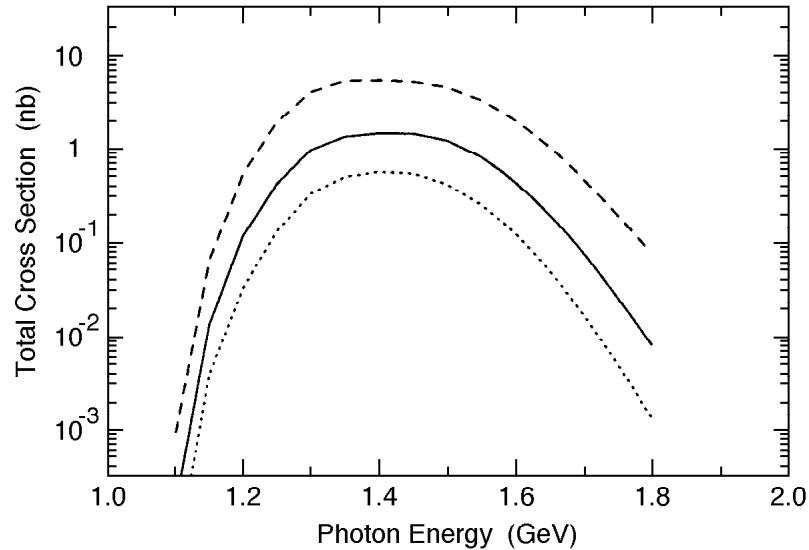


Fig. V-5. The calculated total cross section for the formation of the  $\phi$ -N bound state as a function of the photon energy. The dashed, solid and the dotted curves are for the cutoff  $\Lambda = 2, 3, 4$  fm, respectively.

#### a.20. Compressed Nuclei With $\Delta$ 's and Hyperons (T.-S. H. Lee, Mahmoud A. Hasan,\* and James P. Vary†)

To interpret the data from relativistic heavy-ion collisions, we are continuing our effort to investigate compressed nuclei with  $\Delta$ 's and hyperons. The ground state properties of  $^{90}\text{Zr}$ ,  $^{100}\text{Sn}$ , and  $^{132}\text{Sn}$  at equilibrium and at large amplitude-compression have been investigated within the framework of the constrained spherical Hartree-Fock (CSHF) approximation. We use a realistic effective baryon-baryon Hamiltonian that includes the N-N, the N- $\Delta$  and the  $\Delta$ - $\Delta$  interactions. We specifically investigate the sensitivity to the sizes of the nucleon and  $\Delta$  model spaces. At equilibrium, we find no case of mixing between nucleons and  $\Delta$ 's in our largest model space of eight major nucleon shells plus sixteen  $\Delta$  orbitals. On the contrary, there is mixing in  $^{90}\text{Zr}$ , and  $^{132}\text{Sn}$  in the smaller model space of seven major nucleon shells plus eight  $\Delta$  orbitals. Expanding the nucleon model space has a larger effect on reducing the static compression modulus and softening the nuclear equation-of-state than increasing the number of the  $\Delta$  states. Most of the excitation energy delivered to

the system during compression is employed by the two nuclei with a neutron excess (*i.e.*,  $^{90}\text{Zr}$ ,  $^{132}\text{Sn}$ ) to create the massive  $\Delta$  resonances. On the other hand, in the  $^{100}\text{Sn}$  nucleus, most of the excitation energy goes to a simple reduction in the binding, suggesting a suppressed role for the  $\Delta$  states. Under extreme compression, at a density (2-3) times the normal nuclear density, the excitation of nucleons to  $\Delta$ 's increases sharply up to 10% of the total number of constituents. At finite excitation energy under compression, the number of  $\Delta$  excitations is not dependent on the number of  $\Delta$ -states over the range studied. The  $\Delta$ -excitation results are consistent with heavy-ion collision data, and suggest an important mean-field mechanism for sub-threshold pion production in particle-nucleus and nucleus-nucleus collisions. A paper describing our results has been submitted for publication. We are currently extending the approach to include hyperons in the calculation of compressed nuclei.

\*Applied Science University, Amman, Jordan; †Iowa State University, Ames, IA

### a.21. Medium Effects on $J/\Psi$ Propagation (T.-S. H. Lee, Yongseok Oh,\* and Su Houn Lee\*)

It has been suggested that one of the possible signatures of a quark-gluon plasma (QGP) is the suppression of  $J/\Psi$  production. This can be verified unambiguously only when the propagation of  $J/\Psi$  in hadron matter can be accurately calculated theoretically. In this work, we investigate  $J/\Psi$  propagation in a meson system which could result from the hadronization of a QGP. The starting point of our investigation is a recently developed model<sup>1</sup> for describing  $J/\Psi-\pi$  and  $J/\Psi-\rho$  scattering. Medium effects on the mass of the  $J/\Psi$  are

calculated by integrating the predicted  $J/\Psi-\pi$  and  $J/\Psi-\rho$  scattering amplitudes over the distribution functions of  $\pi$  and  $\rho$ . In contrast with previous work, we will be able to predict not only the imaginary part of the mass, which is related to the dissociation of the  $J/\Psi$  by  $\pi$  and  $\rho$ , but also the real part which is essential in understanding the mass shift of the  $J/\Psi$  spectrum. The medium effects on  $J/\Psi-\pi$  and  $J/\Psi-\rho$  amplitudes will also be included in the calculations.

\*Yonsei University, Japan

<sup>1</sup>Yongseok Oh, Taesoo Song, and Su Houn Lee, Yonsei University preprint nucl-th/0010064 (2000).

### a.22. Dynamical Test of Constituent Quark Models with $\pi N$ Reactions (T.-S. H. Lee, T. Yoshimoto,\* T. Sato,\* and M. Arima†)

A dynamical approach is developed to predict  $\pi N$  scattering amplitudes starting from constituent quark models. The first step is to apply a variational method to solve the three-quark bound state problem. The resulting wave functions are used to calculate the  $N^* \rightarrow \pi N$ ,  $\eta N$ ,  $\pi\Delta$  vertex functions by assuming that the  $\pi$  and  $\eta$  mesons couple directly to quarks. These vertex functions and the predicted baryon bare masses then define a Hamiltonian for  $\pi N$  reactions. We apply a unitary transformation method to derive from the constructed Hamiltonian a multi-channel and multi-resonance reaction model for predicting  $\pi N$  scattering

amplitudes up to  $W = 2$  GeV. With the parameters constrained by the  $\Delta(1232)$  excitation, we have shown that the  $\pi N$  scattering in  $S_{11}$  channel cannot be described by constituent quark models based on the one-gluon-exchange (OGE) or one-meson-exchange (OME) mechanisms. It is found that the data seem to favor the spin-spin interaction due to one-meson-exchange and the tensor interaction due to one-gluon-exchange. A phenomenological quark-quark potential has been constructed to reproduce the  $S_{11}$  amplitude. A paper describing our results has been published.<sup>1</sup>

\*Osaka University, Japan., †Osaka City University, Japan

<sup>1</sup>T. Yoshimoto, T. Sato, M. Arima, and T.-S. H. Lee, Phys. Rev. C **61**, 065201 (2000).

### a.23. Quantum Monte Carlo Calculations of Pion Scattering from Light Nuclei (T.-S. H. Lee, R. B. Wiringa, and C. Fasano\*)

With the development of quantum Monte Carlo methods, it is now possible to evaluate transition densities for the low-lying states of light nuclei. By making use of the strong isospin-dependence of pion-nucleon interaction, we have shown that the predicted relative importance between the neutron and proton transition densities are consistent with the data of pion scattering from  ${}^6\text{Li}$  and  ${}^7\text{Li}$  at energies near the  $\Delta$  resonance. The calculations have been performed by using Distorted Wave Impulse Approximation. The predicted cross sections for  ${}^6\text{Li}$  are compared with the

data in Fig. V-6.. These results and the results for  ${}^7\text{Li}$  have provided a microscopic understanding of the enhancement factors for quadrupole excitations, which were needed to describe pion inelastic scattering within the nuclear shell model. Our results have been published.<sup>1</sup> We are now extending this investigation to test the predictions from quantum Monte Carlo calculations for other light p-shell nuclei. With realistic transition densities, many long-standing problems in  $\pi$ -nucleus scattering will also be investigated.

\*Monmouth College, IL

<sup>1</sup>T.-S. H. Lee and R. B. Wiringa, Phys. Rev. C **63**, 014006 (2001),

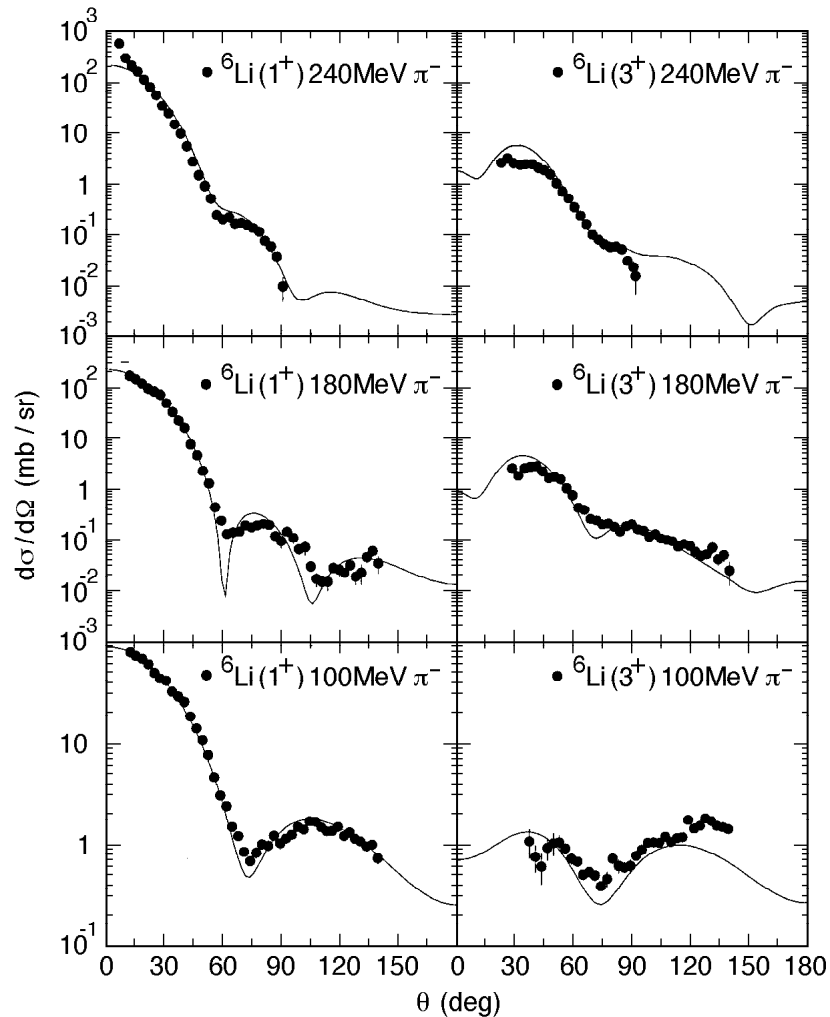


Fig. V-6. Differential cross sections for  ${}^6\text{Li}(\pi,\pi)$  and  ${}^6\text{Li}(\pi,\pi')$  scattering at pion energies  $E_\pi = 100, 180, 240$  MeV.

**a.24. Two Nucleon Correlations in Meson Scattering From  $^{16}\text{O}$**  (B. Mihaila and T.-S. H. Lee)

It has been speculated that the properties of mesons, in particular the vector mesons, can be modified by the nuclear medium. This has motivated some experimental efforts at JLab. To interpret forthcoming data, it is necessary to develop a microscopic description of meson propagation in nuclei. Within the multiple scattering theory, this can be achieved by calculating the meson-nucleus optical potential in terms of meson-nucleon scattering amplitudes and nuclear wave functions. With the correlation functions

generated from the coupled cluster [exp(s)] method,<sup>1</sup> we are investigating this problem by considering meson scattering from  $^{16}\text{O}$ . Our current focus is on the two-nucleon correlation effects in the double scattering term, which plays an important role in determining the meson absorption by nuclei, but is poorly understood. The results will be tested against extensive pion scattering data. Predictions will be made for the propagation of vector mesons in nuclei.

<sup>1</sup>B. Mihaila and J. Heisenberg, Phys. Rev. C **59**, 1440 (1999); **61**, 054309 (2000).

**a.25. Relativistic Quantum Dynamics of Many-Body Systems** (F. Coester and W. N. Polyzou\*)

Relativistic quantum dynamics requires a unitary representation of the Poincaré group on a Hilbert space of states. The dynamics of many-body systems must satisfy cluster separability requirements. An effective realization is based on an auxiliary Hilbert space endowed with a unitary representation of the four-dimensional Euclidean group. A self-adjoint unitary involution operator provides a Poincaré-invariant indefinite inner product. A Euclidean-invariant Green operator specifies the dynamics and the Poincaré-invariant semi-definite inner product of the subspace of

physical states. In this framework two-body Green operators are sufficient to determine many-body Green functions satisfying cluster separability. This approach should be useful in bridging the gap between Hamiltonian particle dynamics based on phenomenological mass operators on one hand and those inspired by quantum field theory on the other. An article on this work will be published by World Scientific in “Advances in Quantum Many-Body Theory”.

\*University of Iowa

**a.26. Null-Plane Dynamics of Elastic Electron Deuteron Scattering** (F. Coester and W.N. Polyzou\*)

It is an inescapable feature of relativistic Hamiltonian dynamics that single-particle current density operators are covariant only under the kinematic subgroup. Null-plane dynamics has the unique feature that, like Galilei covariant dynamics, it allows a consistent impulse approximation, provided the momentum transfer is in the null plane. “Model-independent” interaction currents are introduced by the requirements of rotational covariance. They depend on the angle

between the null vector and the transverse polarization vector used in the computation of form factors. We find that the null-plane impulse approximation provides significantly better agreement with the deuteron data than the Galilei-covariant impulse approximation.<sup>1</sup> Covariant meson-exchange currents<sup>2</sup> can be added consistently in this framework. A quantitative investigation meson-exchange currents is in progress.

\*University of Iowa

<sup>1</sup>R. B. Wiringa V. G. J. Stoks and R. Schiavilla, Phys. Rev. **51**, 38 (1995).

<sup>2</sup>F. Coester and D.O. Riska, Ann. Phys. **234**, 141 (1994).



## B. NUCLEAR FORCES AND NUCLEAR SYSTEMS

The goal of this program is to achieve a description of nuclear systems ranging in size from the deuteron and triton to nuclear matter and neutron stars using a single parameterization of the nuclear forces. Aspects of our program include both the construction of two- and three-nucleon potentials and the development of many-body techniques for computing nuclear properties with these interactions. Detailed quantitative, computationally-intensive studies are essential parts of this program.

Quantum Monte Carlo (QMC) calculations of light ( $A \leq 10$ ) nuclei with realistic interactions have been the main focus of our recent efforts. Our nonrelativistic Hamiltonian contains the accurate Argonne  $v_{18}$  two-nucleon (NN) potential, which includes charge-independence-breaking terms, and either the venerable Urbana IX three-nucleon (3N) potential, or one of several new Illinois NNN models. The QMC calculations include both variational (VMC) and Green's function (GFMC) methods. We begin with the construction of variational trial functions based on sums of single-particle determinants with the correct total quantum numbers, and then act on them with products of two- and three-body correlation operators. Energy expectation values are evaluated with Metropolis Monte Carlo integration and parameters in the trial functions are varied to minimize the energy. These optimized variational wave functions then can be used to study other nuclear properties. They also serve as a starting point for the GFMC calculations, which systematically remove higher excited-state components from the trial wave functions by a propagation in imaginary time.

We are currently studying all  $A \leq 10$  nuclei with experimentally known bound state or resonance energies, including some 55(30) excited states in VMC (GFMC). These are the first and only calculations treating  $A \geq 6$  nuclei directly with realistic NN and NNN interactions. In GFMC calculations, with the new Illinois NNN models, we can reproduce most of the experimental ground- and excited-state energies within 0.5 MeV. The VMC calculations, including two-body charge and current operators, are being used to study weak decays of  $A=6-8$  nuclei and for various  $(e,e'p)$  and  $(e,e'n)$  reactions. They are also being used to obtain astrophysically interesting cross sections, such as  ${}^2\text{H}(d,\gamma){}^6\text{Li}$  and  ${}^3\text{He}(\alpha,\gamma){}^7\text{Be}$ . Finally, we are also studying the properties of neutron drops with the goal of providing additional constraints for the construction of Skyrme interactions that are used in the modeling of neutron-rich nuclei in neutron star crusts.

In addition, a new effort using the coupled cluster [exp(s)] method was initiated this year. The coupled cluster method is being used to study nuclei in the  ${}^{12}\text{C}$ - ${}^{16}\text{O}$  range, using the same realistic Hamiltonian as the quantum Monte Carlo calculations. There will be an opportunity to study some systems, such as  ${}^4\text{He}$  and neutron drops, by both methods, providing a useful check on accuracy. We also are able to compare both methods with results of traditional shell model calculations. Finally, studies of hypernuclei are also continuing, particularly the charge-symmetry-breaking on  $\Lambda\text{N}$  interactions.

### b.1. Quantum Monte Carlo Calculations of Light p-shell Nuclei (S. C. Pieper, K. Varga, R. B. Wiringa, J. Carlson,\* and V. R. Pandharipande†)

Since the early 1990s, we have been studying the ground and low-lying excited states of light p-shell nuclei as A-body problems with realistic nucleon-nucleon (NN) and three-nucleon (NNN) interactions using advanced quantum Monte Carlo (QMC) methods. Our preferred Hamiltonian has been the Argonne  $v_{18}$  NN potential, which gives an excellent fit to elastic NN scattering data and the deuteron energy, and the Urbana IX NNN potential, which was fit to trinucleon energies and the saturation density of nuclear matter. Recently, we have investigated more general NNN potentials, as described in the next section. The QMC methods include both variational Monte Carlo (VMC), which gives an initial approximate solution to the many-body Schrodinger equation, and the Green's function Monte Carlo (GFMC), which systematically improves on the VMC starting point and produces binding energies that are accurate to within 2%. This year our calculations have been extended to A=9,10 nuclei.

The VMC calculations begin with the construction of an antisymmetric Jastrow trial function that includes single-particle orbits coupled to the desired JM values of the state of interest, as well as pair and triplet spatial correlations. It is then acted on by a symmetrized product of two-body spin, isospin, tensor, and spin-orbit correlation operators, induced by the NN potential, and three-body correlation operators for the NNN potential. The wave functions are diagonalized in the small basis of different Jastrow spatial symmetry components to project out higher excited states with the same quantum numbers. A major advance this year was to automate the construction of the different p-shell orbital combinations, which by A=10 have many spatial and spin-isospin symmetries that can contribute.

In the GFMC calculations, we operate on a version of the VMC trial function with the imaginary time propagator,  $\exp[-(H'-E_0)\tau]$ , where  $H'$  is a simplified Hamiltonian,  $E_0$  is an estimate of the eigenvalue, and  $\tau$  is the imaginary time. The excited-state components of the trial function will then be damped out for large  $\tau$ , leaving the exact lowest eigenfunction with the quantum numbers of the input variational wave

function. The expectation value of  $H$  is computed for a sequence of increasing values of  $\tau$  to determine the convergence. Our  $H'$  contains the reprojected  $v_8$  part of the NN potential and the full NNN potential. The small correction  $H-H'$  is computed perturbatively. The many-body propagator is written as a symmetrized product of exact two-body propagators, with the NNN potential treated in lowest order.

In previous years we have made significant improvements in the GFMC algorithms, especially in solving the fermion sign problem for nuclear systems. A major paper detailing the constrained path algorithm, and our results up to A=8 nuclei, was published during the year.<sup>1</sup> As of the beginning of this year, the method and program has been stable and we have concentrated on extending the calculations to larger nuclei and on developing new models of the NNN potential. The computer resources (both CPU time and memory) required for these calculations increase exponentially with the number of nucleons. Therefore progress to bigger nuclei usually requires a new generation of computers.

Two new parallel computers became available to us during this year. We obtained a large amount of early friendly user time on the 256-node IBM SP (each node is a dual-processor RS6000) at NERSC. This was used to make the first GFMC calculations of A=9 nuclei. Using all 512 CPU's, sustained speeds of 100 GFLOPS were obtained. Then the 256-node Linux computer (each node is a dual processor 500-MHz Pentium-3) in Argonne's Mathematics and Computer Science Division became available. Although this machine is slower than the NERSC IBM SP, much more time was available on it and we used it for the first A=10 calculations. Preliminary results from the A=9 and 10 calculations are that the NNN potentials discussed in the next section continue to give generally good predictions of the binding energies, although there is somewhat increased dispersion between the various models that have been made. We do not anticipate quickly going beyond 10 nucleons, but in the next few years A=12 should be attainable.

\*Los Alamos National Laboratory; †University of Illinois, Urbana

<sup>1</sup>R. B. Wiringa, Steven C. Pieper, J. Carlson, and V. R. Pandharipande, Phys. Rev. C **62**, 014001 (2000).

## b.2. Studies of Three-Nucleon Interactions in Nuclear Systems (S. C. Pieper, R. B. Wiringa, V. R. Pandharipande\*, D. G. Ravenhall,\* and J. Carlson†)

Our GFMC calculations of nuclei with  $3 \leq A \leq 8$  using the Hamiltonian consisting of the Argonne  $v_{18}$  two-nucleon (NN) and Urbana IX three-nucleon (NNN) potentials have shown that this Hamiltonian underbinds p-shell nuclei by 0.8 MeV in  ${}^6\text{Li}$  to 5 MeV in  ${}^8\text{He}$ . The error increases with both  $A$  and  $|N-Z|$ . In the last few years, we have been constructing improved “Illinois” models for the NNN potential.

Our approach is to use theoretical guidance to suggest the structure of new terms, but to consider the coupling constants and short-range shapes of the potential to be adjustable. This is in the same spirit as the development of realistic NN potentials. We have considered a number of new terms. We find that new potential terms are often not perturbative, *i.e.*, an expectation value of the new term using the GFMC wave function from just Argonne  $v_{18}$  and Urbana IX may be misleading. Thus each new term must be added to the GFMC propagator and a new GFMC calculation made. Furthermore, as the strength of the new term is adjusted, the propagations must be repeated.

The dominant term of the Urbana potential is the Fujita-Miyazawa (FM) two-pion term with intermediate excitation of one nucleon to a  $\Delta$ . We have now studied three-pion ring terms containing one and two  $\Delta$  excitations. These are repulsive in s-shell nuclei and attractive in p-shell nuclei and correct the overall loss

of binding energy with respect to both  $A$  and  $|N-Z|$ . The Tucson-Melbourne potential contains the FM term and a two-pion term arising from s-wave  $\pi N$  scattering; we have also considered a corrected s-wave term.

The FM terms in the Urbana NNN potentials and the new models that we first constructed have coupling constants that are about 1/2 the value suggested by soft pion physics. We have also made a model that has the stronger coupling constant; this required a significantly softer cutoff parameter (normally we use the same cutoff as is used in the NN potential). Most of the models have the two-pion s-wave term with the strength preferred by chiral perturbation theory, but one of the models omits this term. In all five Illinois models have been developed with various strengths for the four potential terms. All of them give excellent fits to the  $3 \leq A \leq 8$  binding energies— the rms errors are  $\leq 500$  keV. However, there is more dispersion in the quality of fit to the 9- and 10-body nuclei. Preliminary calculations of nuclear matter with these potentials also show significant differences between the models. Figure V-7 compares GFMC values of ground and excited state energies for Argonne  $v_{18}$  with no NNN potential and one of the new Illinois models to experimental values. One sees the very important contributions made by the NNN potential to the p-shell binding energies, and the generally very good resulting agreement with the data.

---

\*University of Illinois, Urbana, †Los Alamos National Laboratory

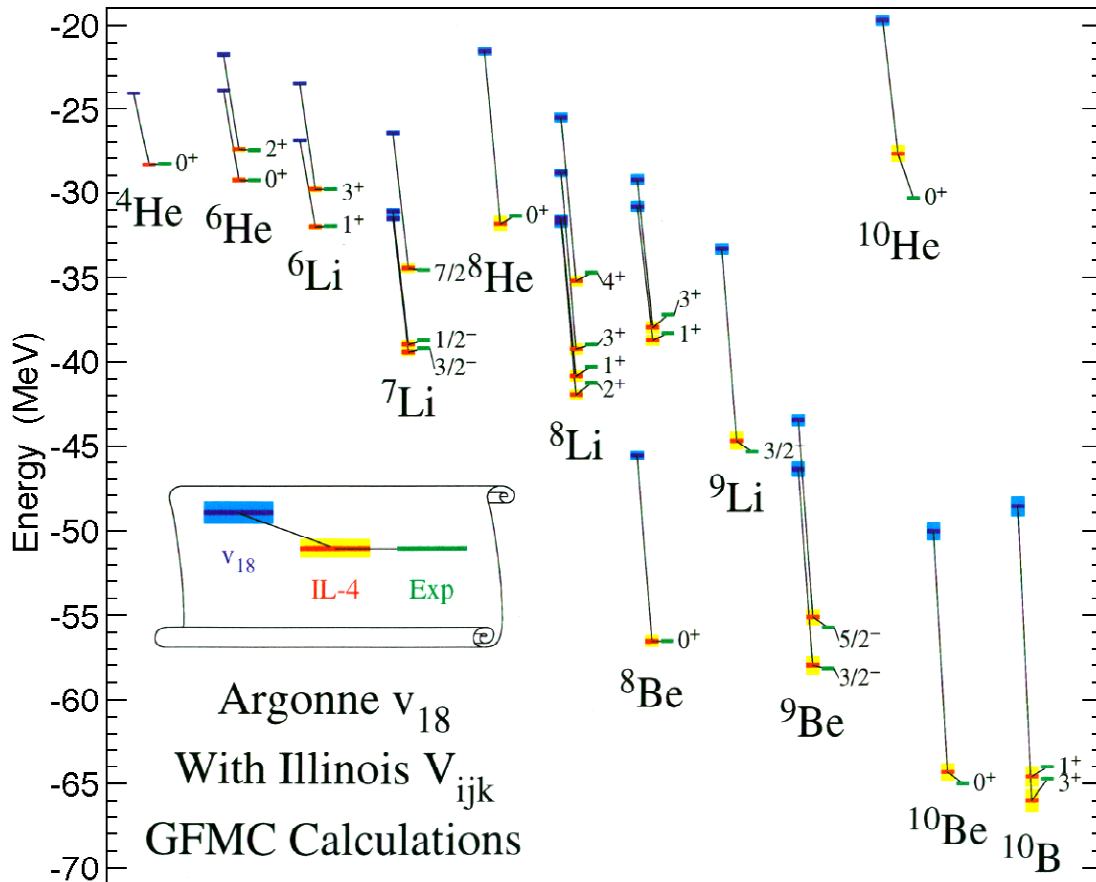


Fig. V-7. GFMC energies for  $A=4-10$  nuclei using the Argonne  $v_{18}$  NN potential by itself and with one of several new Illinois NNN potentials, compared to experiment.

### b.3. Radiative Capture Reactions for Astrophysical Applications (K. M. Nollett, R. B. Wiringa, and R. Schiavilla\*)

Radiative capture reactions play a major role in many astrophysical processes, including primordial nucleosynthesis and stellar evolution. We have used the many-body variational Monte Carlo wave functions discussed above to study several capture reactions involving light p-shell nuclei. The first project was to obtain the low-energy cross section for  ${}^2\text{H}(\alpha,\gamma){}^6\text{Li}$ , which is the primary source of  ${}^6\text{Li}$  in the big bang. While  ${}^2\text{H}$ ,  ${}^3\text{He}$ ,  ${}^4\text{He}$ , and  ${}^7\text{Li}$  are dominant nuclei synthesized in the big bang, trace amounts of  ${}^6\text{Li}$  should also have been made. Astronomical searches are being made in an attempt to detect primordial  ${}^6\text{Li}$ , but results are ambiguous at present. The cross section at keV energies is sufficiently small that direct laboratory measurements have only established an upper bound, while the analysis of indirect experiments is problematic.

We evaluate the appropriate matrix elements (primarily E1 and E2) between the  ${}^6\text{Li}$  ground state and a correlated  $\alpha+d$  pair, which is then folded with a continuum  $\alpha+d$  wave function obtained from one of the suitable optical potentials found in the literature. The problem factorizes into a one-dimensional energy-dependent integral and a multi-dimensional energy-independent kernel. The latter is over the coordinates of all the particles and requires significant computation, but it needs to be evaluated only once for any given partial wave. The outer integral, over the  $\alpha+d$  separation, can then be evaluated for any number of energies at little additional cost. An important ingredient in the calculation was the development of a new variational wave function for the  ${}^6\text{Li}$  ground state

which has the correct  $\alpha+d$  cluster structure at long ranges.

Our result, calculated with the VMC wave functions for the Argonne  $v_{18}$  + Urbana IX Hamiltonian, is shown in Fig.V-8 for two different choices of the  $\alpha+d$  optical potential, where it is compared to the experimental data. The reaction is a mixture of E1 and E2 contributions, with E2 dominating from just below the  $3+$  resonance to beyond 3 MeV. However, the E1 contribution, which comes about as a relativistic center-of-energy term, dominates at the low energies (20-200 keV) which are important for the big bang. An important advantage of this work is the ability to evaluate small terms like this in a fully correlated many-body wave function. A paper describing this work has been accepted for publication in Physical Review C.<sup>1</sup>

The second project was to study the  ${}^3\text{H}(\alpha,\gamma){}^7\text{Li}$  and  ${}^3\text{He}(\alpha,\gamma){}^7\text{Be}$  capture reactions, which both contribute to primordial nucleosynthesis, while the latter is also important for solar neutrino production. These reactions can be measured in the laboratory at the low energies of interest, but absolute normalizations are difficult to control and the S-factor for  ${}^7\text{Be}$  has a  $\pm 20\%$  experimental uncertainty. In both of these reactions, the captures can take place to either the  $3/2^-$  ground

state or the  $1/2^-$  excited state, and experimental branching ratios are also available.

Again, external optical potentials for the  $4+3$  scattering wave functions were taken from the literature. However, for these cases, there was a significantly greater variation in the results depending on which optical potential was used. The best led to a  ${}^7\text{Li}$  S-factor in good agreement with the data, although the branching ratio was low, while the  ${}^7\text{Be}$  S-factor is a few % below the lowest data, but with a better branching ratio. In all cases, the energy dependence of the results was very good.

This latter work was the University of Chicago Ph.D. thesis for Ken Nollett, and has been submitted to Physical Review C. The calculations can be improved in the future by: 1) using the more accurate GFMC wave functions for the ground states, particularly the p-shell nuclei; 2) using the better Illinois three-nucleon potentials discussed above instead of the Urbana IX, which slightly underbinds the p-shell nuclei; and 3) using GFMC techniques to develop consistent  $\alpha$ -cluster scattering states from the bare interactions instead of relying on an optical potential. It should also be possible to extend these calculations in the near future to additional reactions of interest such as  ${}^7\text{Be}(p,\gamma){}^8\text{B}$ .

\*TJNAF and Old Dominion University

<sup>1</sup>K. M. Nollett, R. B. Wiringa, and R. Schiavilla, Phys. Rev. C **63**, 024003 (2001).

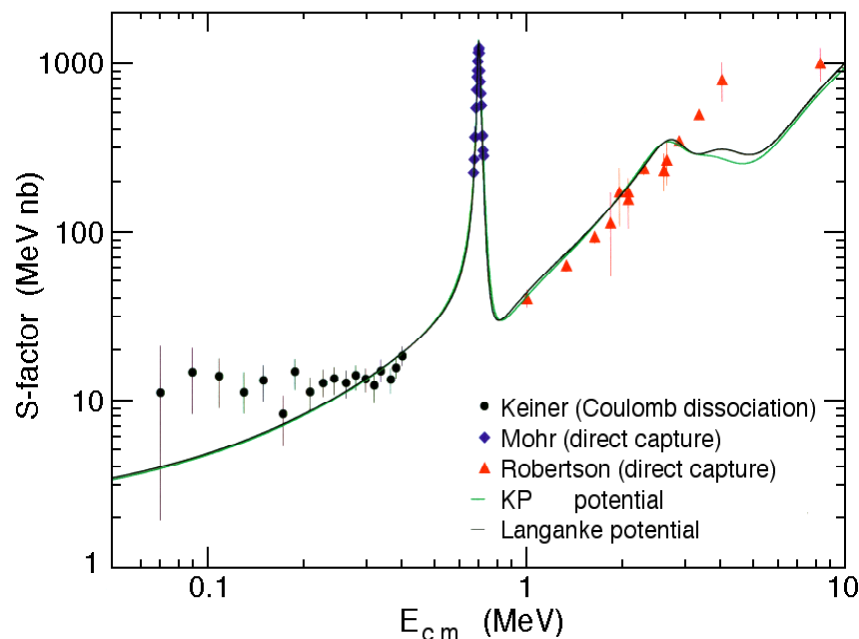


Fig. V-8.. The total s-factor for  $\alpha+d$  radiative capture calculated for two different optical potentials with the AV18/UIX nuclear wave functions, compared to experimental data.

#### b.4. Microscopic Calculation of A = 6–8 Weak Decays (R. B. Wiringa, S. C. Pieper, and R. Schiavilla\*)

Initial quantum Monte Carlo calculations have been made for the weak decays of  ${}^6\text{He}$ ,  ${}^7\text{Be}$ ,  ${}^8\text{He}$ ,  ${}^8\text{Li}$ , and  ${}^8\text{B}$ . Variational wave functions were obtained for our standard Hamiltonian containing the Argonne  $v_{18}$  two-nucleon potential and the Urbana IX three-nucleon potential. Consistent two-body axial current operators tuned to reproduce  ${}^3\text{H}$   $\beta$ -decay are included in the evaluations.

Our calculated Gamov-Teller (GT) matrix element for  ${}^6\text{He}(\beta^-){}^6\text{Li}$  is about right, while those for  ${}^7\text{Be}(\epsilon){}^7\text{Li}$  and  ${}^7\text{Be}(\epsilon){}^7\text{Li}^*$  are 5% too low, compared to experiment. The two-body axial current contributes only a 1% increase in A=6 and 3% in A = 7. The branching ratio  ${}^7\text{Li}^*/{}^7\text{Li}$  is 10.2% compared to the experimental 10.5%. We are currently studying the sensitivity of these results to changes in the variational wave function, and have started to evaluate mixed estimates with the more precise GFMC wave functions and use the new Illinois three-nucleon potentials. At present, the status of these *ab initio* calculations of A = 6–7 weak decays looks quite satisfactory.

\*TJNAF and Old Dominion University

#### b.5. Coupled Cluster Expansion Approach to Calculating Ground State Properties of Closed Shell Nuclei in the p-Shell (Bogdan Mihaila and Jochen Heisenberg\*)

We investigate the ground state properties of closed shell nuclei in the p-shell using the coupled-cluster expansion [exp(s)] method. We solve the many-body Schroedinger equation with a nonrelativistic Hamiltonian based on the Argonne  $v_{18}$  two-nucleon interaction, supplemented with the Urbana IX three nucleon interaction. In this framework we extend our previous

\*University of New Hampshire

The situation for A=8 weak decays is much more difficult. While the A=6–7 decays are between states of predominantly the same spatial symmetry, the  ${}^8\text{Li}$  and  ${}^8\text{B}$  decays involve transitions from the  $2^+[31]$  ground states to the  $2^+[4]$  first excited state of  ${}^8\text{Be}$ , which is in fact a fairly broad resonance.

The impulse approximation gives only 39% of the experimental GT matrix element; the two-body axial current is relatively more important here, but only boosts our result to 43%. The  ${}^8\text{He}(\beta^-){}^8\text{Li}$  decay proceeds from the  $0^+[22]$  ground state to several  $1^+[31]$  excited states. Again, we get less than 50% of the measured GT matrix element to the lowest  ${}^8\text{Li}$  state; however, in the  ${}^8\text{He}$  decays, the experimental data is less complete. We will be investigating alternate variational wave functions and computing GFMC mixed estimates in the near future. However, these suppressed A=8 decays will probably require additional physics input to reach a satisfactory state.

results for the ground state of  ${}^{16}\text{O}$ , to the calculation of  ${}^{12}\text{C}$ ,  ${}^{14}\text{C}$  and  ${}^{14}\text{O}$ . The calculation results involve the binding energies of the above nuclei, together with the one- and two-body densities in the ground state. The densities allow for the microscopic calculation of electron scattering structure functions and corrections for the center-of-mass motion.

### b.6. Coupled Cluster Calculation for Single Particle States and the Magnetic Form Factor (Bogdan Mihaila and Jochen Heisenberg\*)

We extend the coupled-cluster expansion formalism to the calculation of ground state and excited Yrast states of single-hole nuclei. The approach is based on the prior knowledge of ground state correlations of a related spherically symmetric, double-closed-shell nucleus. As such, we infer the properties of  $^{11}\text{B}$ ,  $^{13}\text{C}$

and  $^{15}\text{N}$ , based on our previous calculations for the ground states of  $^{12}\text{C}$ ,  $^{14}\text{O}$ , and  $^{16}\text{O}$ , respectively. We calculate the elastic magnetic form factors for  $^{15}\text{N}$  and  $^{13}\text{C}$ , and compare with the existing electron scattering experimental data.

---

\*University of New Hampshire

### b.7. Meson Exchange Effects in p-Shell Nuclei (Bogdan Mihaila and Jochen Heisenberg\*)

The modeling of the large momentum behavior of magnetic and electric form factors as obtained via electron scattering experiments on p-shell nuclear targets is a long standing problem in theoretical nuclear physics. Here one has to entangle effects of the nuclear interaction, nuclear correlations, meson-exchange contributions and relativistic effects. At this stage of the project we seek to accurately calculate the meson-

exchange charge and current density contributions using the nuclear correlations obtained via the coupled-cluster method together with a nonrelativistic Hamiltonian with realistic nuclear interactions. We compare various models available today, and investigate the importance of having a realistic meson-exchange model consistent with the NN interaction model.

---

\*University of New Hampshire

### b.8. Comparison of M1 and E1 Properties for Light 1p-shell Nuclei (D. Kurath)

Recently Monte Carlo calculations with a realistic Hamiltonian have produced energy spectra in close agreement with experimental observations. Previously a 1p shell model had been fitted to low-lying energy levels to derive an effective two-body interaction together with single particle levels with respect to  $^4\text{He}$ . The resultant wave functions can be used to derive electromagnetic properties for these nuclei.

The choice of interactions for the Monte Carlo case is the Argonne  $v_{18}$  2-body interaction plus the Illinois2

(IL2) 3-body interaction as used in Green's Function (GFMC) calculations. For the shell model we use the (6-16 2B) interaction of Cohen and Kurath (CK). For the magnetic dipole cases no effects of mesonic currents are included and free nucleon values are used for the neutrons and protons. In the case of E2 transitions the shell model calculations include effective charges  $e_p=1.4e$  and  $e_n=0.4e$  to represent deformation not included in the 1p space. In Table 1, M1 moments of ground states are compared to experiments.

Table V-1. Magnetic Moments in Nuclear Magnetons

NUCLEUSs	J	EXP	IL2	CK
${}^6\text{Li}$	1	0.822	0.817	0.833
${}^7\text{Li}$	1.5	3.256	2.86	3.170
${}^7\text{Be}$	1.5	-1.398	-1.07	-1.289
${}^8\text{Li}$	2	1.653	0.91	1.556
${}^8\text{B}$	2	1.036	1.65	1.095
${}^9\text{Li}$	1.5	3.439	2.5	3.375
${}^9\text{C}$	1.5	-1.391	-0.8	-1.483
${}^9\text{Be}$	1.5	-1.178	-1.14	-1.268
${}^9\text{B}$	1.5	--	2.92	3.082

The isoscalar contribution is represented by half the sum of the moments of mirror nuclei while  $1/(2*t_z)$  times the difference gives the isovector contribution.

Table V-2. Isoscalar and Isovector Contributions

MASS	T	ISOSCALAR		ISOVECTOR			
		EXP	IL2	CK	EXP	IL2	CK
7	1/2	0.929	0.895	0.940	-4.654	-3.93	-4.459
8	1	1.344	1.280	1.326	-0.309	+0.37	-0.230
9	3/2	1.024	0.850	0.946	-1.610	-1.10	-1.619
9	1/2	--	0.890	0.907	--	+4.06	+4.350

The isoscalar contributions are quite similar in all three rows, but the isovector contributions in the IL2 case are considerably different in the first three rows. Mesonic contributions can affect these isovector terms, but it is then puzzling why they do not seem necessary in the shell model cases.

Electric multipole operators are sensitive to radial distributions, and the shell model is given effective charges for neutrons and protons which are however fixed at  $e_p=1.4e$  and  $e_n=0.4n$  for all nuclei here, together with  $\langle r^2 \rangle = 7.06 \text{ fm}^2$ .

Table V-3. Electric Quadrupole Moments in Units of  $e\text{-fm}^2$ 

NUCLEUS	J	EXP	IL2	CK
${}^6\text{Li}$	1	-0.083	-0.32	-1.33
${}^7\text{Li}$	3/2	-4.02	-3.61	-3.76
${}^7\text{Be}$	3/2	--	-6.10	-5.28
${}^8\text{Li}$	2	+3.20	+3.19	+2.92
${}^8\text{B}$	2	+6.6	+6.43	+4.38
${}^9\text{Li}$	3/2	-2.74	-2.71	-4.02
${}^9\text{C}$	3/2	--	-8.68	-3.75
${}^9\text{Be}$	3/2	+5.29	+8.52	+4.58
${}^9\text{B}$	3/2	--	+8.74	+3.32
${}^{10}\text{B}$	3	+8.47	+9.53	+8.65



On the whole the IL2 values are much closer to experiment, reflecting the ability of the Monte Carlo calculations to give the effect of binding energy on the radial functions.

Finally, we present some E2 and E4 properties of  ${}^8\text{Be}$  as given by IL2 and CK compared to the results of a rotational model. In this model  ${}^8\text{Be}$  is represented by a  $K=0$  rotational band and all transitions are related by Clebsch-Gordan coefficients to intrinsic E2 or E4 moments.

Table V-4. E2 and E4 Properties of  ${}^8\text{Be}$  for the ROT Model  $Q_{20} = 8.5 \text{ efm}^2$  and  $Q_{40} = 39 \text{ e-fm}^4$

	ROT	IL2	CK
BE2(2→0)	14.5	14.8	14.2
BE2(4→2)	20.6	18.2	12.7
<EQ>(J=2)	-7.7	-7.6	-7.9
<EQ>(J=4)	-9.8	-9.8	-9.6
BE4(4→0)	169	166	
<E4>(J=2)	1.9	2.5	
<E4>(J=4)	4.9	4.9	

Thus  ${}^8\text{Be}$  is calculated to be a good rotational nucleus.

### b.9. Studies of Hypernuclei (A. R. Bodmer, Q. N. Usmani, and Rita Sinha\*)

We are continuing our studies of hypernuclei. In particular, we are revisiting the mass  $-4$  hypernuclei,  ${}^4_\Lambda\text{H}$  and  ${}^4_\Lambda\text{He}$ , with respect to the  $\Lambda$ -nucleon ( $\Lambda\text{N}$ ) charge-symmetry-breaking interaction. Some time ago we studied this question using central nucleon-nucleon

(NN) potentials and found that the  $\Lambda\text{N}$  charge-symmetry-breaking potential was effectively spin-independent. We intend using realistic NN potentials which include non-central components, and three-nucleon potentials which could modify this conclusion.

\*Universiti Putra Malaysia

### b.10. Neutron-Proton Density Differences in Nuclei (A. R. Bodmer and Q. N. Usmani\*)

We are studying the neutron and proton densities in nuclei in a local density approach. Our emphasis is on the density difference whose behavior we can effectively separate out from that of the total density. In particular, in addition to the dependence on the neutron excess which is explicit, we have identified the density dependence of the symmetry – energy density

as the main determinant of the difference between the neutron and proton densities. This is consistent with a very old result obtained by one of us (ARB). The surface symmetry energy can also be explicitly identified and is closely related to the neutron-proton density difference. This work is actively in progress.

\*Universiti Putra Malaysia

### C. NUCLEAR STRUCTURE AND HEAVY-ION REACTIONS

This research focuses on nuclear structure in unusual regimes: nuclei far from stability, and superdeformed nuclei at high spin. We also study heavy-ion reactions near the Coulomb barrier. Much of this work is closely tied to experiments performed at ATLAS and at radioactive beam facilities.

Our studies of drip-line nuclei focus on breakup reactions, induced by the Coulomb and nuclear fields from a target nucleus. A critical issue is to develop a realistic description of the breakup mechanisms as a necessary tool for extracting nuclear structure properties of drip-line nuclei. We have developed a numerical technique to calculate the time evolution of the wave function for the relative motion of a halo nucleon and a core nucleus in the time-dependent fields from a target nucleus. We have used this technique to test the much simpler eikonal approximation, which is commonly used to calculate the nuclear induced breakup.

We have completed the analyses of  $^8\text{B}$  Coulomb dissociation experiments and extracted the low-energy E1 strength. From this we infer an S-factor for the radiative proton capture on  $^7\text{Be}$  that is consistent with direct capture measurements. The consistency demonstrates that the Coulomb dissociation method is a viable technique, which is particularly useful in cases where direct capture measurements are difficult.

Our studies of the proton decay from nuclei beyond the proton drip-line is based on a coupled-channels technique. We have developed an efficient and reliable method to calculate the extremely narrow decay widths of interest. We have applied our methods to the decay from deformed nuclei, based on a particle-rotor Hamiltonian model. The results we obtain for the total decay width and the branching ratio to the  $2^+$  excited state of the daughter nucleus are quite encouraging in comparison to measurements for  $^{131}\text{Eu}$ . We have also applied our methods to near-spherical nuclei, using a particle-vibration Hamiltonian model.

Our studies of superdeformation at both low and high spins address the issue of possible new regions of superdeformation and hyperdeformation. Special emphasis is being put on the study of fission barriers at high spin as this is crucial for the possible production of very extended nuclei. Other areas of interest are the structures of heavy elements and superheavy elements, proton radioactivity, nuclear structure in the neutron deficient Pb region and neutron-proton pairing near the  $N=Z$  line. The techniques that we use to study these problems are: 1) the Strutinsky method coupled with a deformed Woods-Saxon, mean field, 2) self-consistent mean field calculations using the Gogny interaction, and 3) many-body wave functions where mean-field approaches are inadequate.

Much of this work is computer intensive and we have adapted many of our codes to exploit the massively parallel IBM SP and Chiba computer systems at Argonne. By parallelizing our codes, we are able to study nuclei as a function of angular momentum in a four-dimensional shape space using the Strutinsky method with cranking. We have studied nuclides with masses ranging from  $A\sim 80$  to  $A\sim 200$  with this approach. The calculations suggest several nuclides that are promising candidates for finding superdeformed and hyperdeformed shapes.

By exploiting the parallelization features of these computer systems, we have been able to speed up each iteration in our many-body variational code by a factor of five. This has allowed us to make detailed studies of the nuclides in the neutron-poor Pb region. Our calculations, in conjunction with studies by J. L. Egido and L.M. Robledo, suggest the existence of many low-lying  $0^+$  excited states in this region. Experimental searches for these states are being carried out.

Together with I. Ahmad, we have completed analyses of spectroscopic studies in  $^{256}\text{Fm}$  and  $^{251}\text{Cf}$ . The single-particle level spacings and pairing interaction strengths obtained from these analyses will be useful for studies of energy surfaces in superheavy elements. Many of the deformed orbitals seen in these nuclides have large components of the spherical levels near the Fermi level of superheavy elements.

### c.1. Coupled-channels Treatment of Deformed Proton Emitters (H. Esbensen and C. N. Davids)

We have developed a numerical technique to calculate the wave function and decay width of proton decaying states in heavy, deformed nuclei.<sup>1</sup> We adopt a particle-rotor model, with a proton interacting with a deformed, even-even core nucleus. The wave function  $\Psi_1$  of a decaying state is expanded on the channel-spin wave functions  $[|lj\rangle|R\rangle]_1$ , where a single-particle orbit  $|lj\rangle$  is coupled to a rotational state  $|R\rangle$  of the core nucleus to form the total spin  $I$  of the decaying state, *i.e.*,

$$\Psi_1 = \sum_r \frac{\phi_{ljR}(r)}{r} [|lj\rangle|R\rangle]_1.$$

The radial wave functions  $\phi_{ljR}(r)$  are calculated in a coupled-channels approach. For the extremely narrow widths of interest ( $\approx 10^{-20}$  MeV), the asymptotic boundary conditions can be expressed in terms of irregular Coulomb wave functions as  $\phi_{ljR}(r) = N_{ljR}G_1(k_R r)$ , where  $hk_R$  is the momentum of the emitted proton. The amplitude  $N_{ljR}$  determines the associated partial decay width,  $\Gamma_{ljR} = h^2 k_R / m |N_{ljR}|^2$ .

One difficulty in calculating the wave function of a decaying state is to include the influence of the long-ranged Coulomb quadrupole interaction. We have overcome this problem simply by solving the coupled equations inside the nuclear interaction region and then estimating the influence of the long-ranged Coulomb couplings to first order using a Green's function

technique. We find that this method converges quite rapidly.

We have used our methods to analyze the proton decay from the  $3/2^+$  ground state of  $^{131}\text{Eu}$ , which has been measured at ATLAS, both to the ground state and to the  $2^+$  excited state of the daughter nucleus  $^{130}\text{Sm}$ . The decay to the ground state involves the emission of a  $d_{3/2}$  proton orbit. This component of the decaying state is small. The dominant component is a  $d_{5/2}$  orbit, which is coupled to the  $2^+$  state of the core. We find that the branching ratio of the two observed decay modes is very sensitive to deformation in the spin-orbit force. Moreover, we are able to reproduce the measurement<sup>2</sup> with a spin-orbit strength that is commonly used in this mass region.

We also applied our methods to analyze the proton decay from the  $7/2^-$  ground state of  $^{141}\text{Ho}$ . We find in this case a decay width that is 3 times smaller than has been measured.<sup>3</sup> We ascribe the discrepancy to Coriolis mixing, which is quite strong in this case. In fact, we obtain a much more realistic decay width in the adiabatic limit, where the rotational energy of the core is set to zero and Coriolis mixing vanishes. In order to obtain a realistic result in the full coupled-channels treatment, one would need to attenuate Coriolis mixing, for example, by implementing the effect of pairing. This work has been published.<sup>1</sup>

<sup>1</sup>H. Esbensen and C. N. Davids, Phys. Rev. C **63**, 014315 (2001).

<sup>2</sup>A. A. Sonzogni *et al.* Phys. Rev. Lett. **83**, 1116 (1999).

<sup>3</sup>C. N. Davids *et al.*, Phys. Rev. Lett. **80**, 1849 (1998).

### c.2. **Vibrational Interpretation of Spherical and Near-Spherical Proton Emitters** (C. N. Davids and H. Esbensen)

There has been a recent observation of fine structure in the proton decay of  $^{145}\text{Tm}$ .<sup>1</sup> The ground-state and fine structure groups have energies of 1.728 MeV and 1.404 MeV, respectively, yielding an excitation energy of 0.326 MeV for the first  $2^+$  state in the daughter nucleus  $^{144}\text{Er}$ . The  $2^+$  branching ratio is 12%. If this were a deformed nucleus, it would imply a deformation of  $\beta_2 \approx 0.18$ , but calculations in the adiabatic limit for these conditions cannot reproduce either the half-life or the branching ratio, for states near the Fermi surface having  $1/2 \leq J \leq 11/2$ .

This suggests that another approach be tried, namely, to consider the daughter nucleus to be vibrational in nature, rather than permanently deformed. We have

modified our coupled-channels formalism<sup>2</sup> to include vibrational couplings in the single-particle Hamiltonian, along with spherical Coulomb and spin-orbit terms. The calculations are done to first order in the vibrational parameter  $\alpha_0$ , which can be related empirically to the excitation energy of the  $2^+$  state. We use the same optical potential parameters as were used in Ref. 2. Assuming a total spin of  $11/2^-$  we obtain remarkable agreement with both the total and the partial proton decay widths of  $^{145}\text{Tm}$ , as well as for the decay widths of other spherical proton emitters.

We have begun to extend the calculations to include pairing, using the BCS formalism. This allows a more realistic spectroscopic factor to be calculated.

<sup>1</sup>K. Rykaczewski, presented at NS2000, E. Lansing, MI, August 2000.

<sup>2</sup>H. Esbensen and C. N. Davids, Phys. Rev. C **63**, 014315 (2001).

### c.3. **Accuracy of Eikonal Model of Fragmentation Reactions** (H. Esbensen and G. F. Bertsch\*)

A wide variety of reaction models have been developed and applied to analyze breakup reactions of halo nuclei at intermediate and high energies. A convenient model of the nuclear induced breakup is the eikonal approximation which is well justified at high energies. Many fragmentation experiments have been performed in the energy range of 20-60 MeV per nucleon. It is therefore of interest to see how accurate the eikonal approximation is in this energy range and at which energy it becomes unreliable.

We have tested the eikonal approximation by comparing it to solutions of the time-dependent Schroedinger equation, where we numerically follow the time evolution of the wave function for the relative motion of a halo nucleon and a core nucleus, under the influence of the nuclear field from a target nucleus. We take  $^{11}\text{Be}$  as a typical example and use standard optical potentials to describe the interaction with the target.

We compare the one-neutron removal probabilities that we obtain from the two methods, and also the two separate components from stripping and diffraction dissociation.

We first tested our numerical techniques by comparing the results at 400 MeV per nucleon on a  $^{12}\text{C}$  target. We found that the eikonal approximation reproduced both the stripping and diffraction dissociation probabilities of the full dynamical calculation to better than 2%. Next, we calculated the breakup probabilities as functions of the beam energy. A typical set of results is illustrated in Fig. V-9 for an impact parameter of 8 fm. The solid curve is the ratio of the one-neutron removal probability that we obtain in the eikonal approximation and in the full calculation, respectively. It is seen that the eikonal approximation gets worse as the energy is reduced to 20 MeV per nucleon, where the discrepancy is 25%.

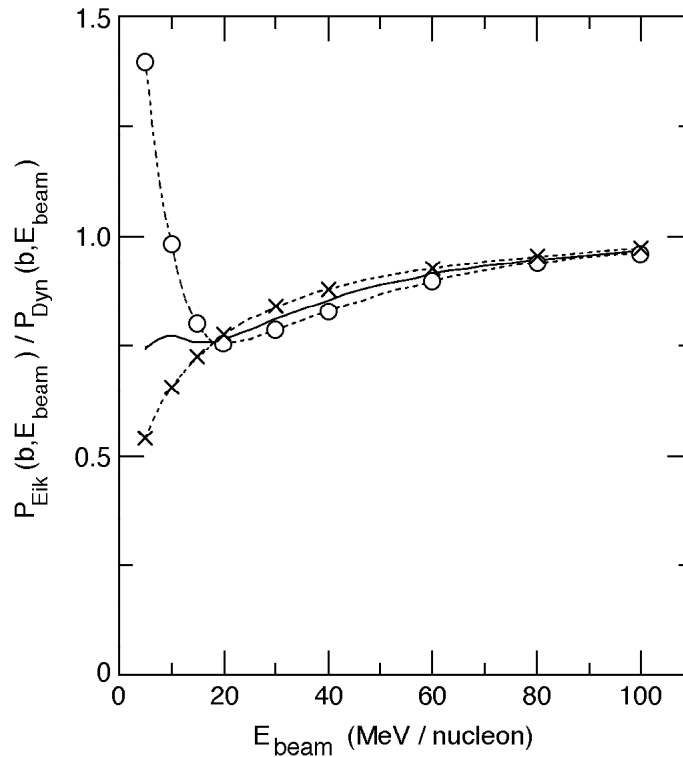


Fig. V-9. Ratios of  $^{11}\text{Be} \rightarrow ^{10}\text{Be} + n$  breakup probabilities, obtained in the eikonal approximation and the time-dependent Schroedinger equation at an impact parameter of 8 fm on a  $^{12}\text{C}$  target, are shown as functions of the beam energy. The solid curve is the ratio of the total one-neutron removal probabilities. The results for stripping (x) and diffraction dissociation (o) are connected by dashed lines.

In Fig. V-9 we also show the same ratios for stripping (x) and diffraction dissociation (o). It is seen that the two components behave in a similar way down to 20 MeV per nucleon, although the stripping component is slightly better predicted by the eikonal approximation.

Below 20 MeV per nucleon, however, both components are poorly described by the eikonal approximation. We intend to investigate the target dependence and also to compare the final state momentum distributions that the two approaches predict. This work is in progress.

\*INT, University of Washington, Seattle

#### c.4. Analyses of $^8\text{B}$ Coulomb Dissociation Experiments (H. Esbensen, B. Davids,\* and others\*)

We have completed our analyses of  $^8\text{B}$  Coulomb dissociation experiments. In the latest experiment,<sup>1</sup> the momenta of the emitted proton and the  $^7\text{Be}$  fragment were recorded in coincidence, which allowed us to construct the decay-energy spectrum of the Coulomb excited  $^8\text{B}$ . The experiment was performed at 83 MeV per nucleon, and the data were analyzed for  $^8\text{B}$  scattering angles that are less than  $1.8^\circ$ , which corresponds to impact parameters larger 30 fm. The large beam energy and small scattering angles were chosen in order to reduce the contributions from E2 transitions and nuclear induced breakup.

We have previously deduced the E2 strength of  $^8\text{B}$  from measurements of the asymmetry in the longitudinal momentum distributions of  $^7\text{Be}$  fragments.<sup>2</sup> From the

deduced E2 strength, and also the known M1 strength, we estimate that E1 transitions dominate our measured decay-energy spectrum by more than 90%, except for relative energies below 130 keV and a narrow energy range around the M1 resonance. Using first-order perturbation theory we could then extract the E1 strength by fitting the measured decay-energy spectrum. Using detailed balance we could finally infer the S-factor for the radiative proton capture on  $^7\text{Be}$ . The best fit in the relative energy range of 130-400 keV yielded an S-factor of  $17.8 \pm 1.4/-1.2$  eV b, whereas a fit up to 2 MeV gave a slightly higher S-factor of  $19.1 \pm 1.5/-1.8$  eV b. The data and the two fits are shown in Fig. V-10. Our results for the S-factor are consistent with a direct capture measurement<sup>3</sup> ( $18.4 \pm 2.2$  eVb). This work has been accepted for publication.<sup>1</sup>

\*Michigan State University, E. Lansing

<sup>1</sup>B. Davids *et al.*, Phys. Rev. Lett. (in press, 2001).

<sup>2</sup>B. Davids *et al.*, Phys. Rev. Lett. **81**, 2209 (1998).

<sup>3</sup>B. W. Filippone *et al.*, Phys. Rev. C **28**, 2222 (1983).

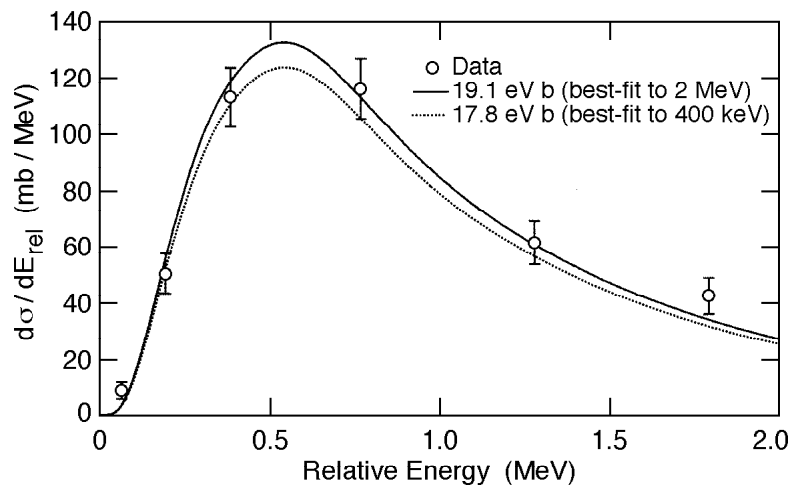


Fig. V-10. Measured cross section for the Coulomb dissociation of 83 MeV/nucleon  $^8\text{B}$  on Pb with  $^8\text{B}$  scattering angles  $\leq 1.8^\circ$ . Only relative errors are shown. Also depicted are the best-fit first-order perturbation theory calculations for the data between 130 keV and 2 MeV, and for the data between 130 keV and 400 keV, convoluted with the experimental resolution. The data point at 64 keV was excluded from the fit because of a large E2 contribution.

### c.5. Giant Resonances in Exotic Nuclei (H. Esbensen and H. Sagawa\*)

We discuss characteristic features of Giant Dipole (GDR) and Giant Quadrupole (GQR) Resonances in nuclei far from stability.<sup>1</sup> Experimental studies have so far focused on determining the dipole strength of light halo nuclei. By measuring the decay-energy spectrum produced in Coulomb dissociation experiments, it has been possible to extract a large dipole strength near threshold in halo nuclei such as  $^6\text{He}$ ,  $^8\text{He}$ ,  $^{11}\text{Li}$ ,  $^{11}\text{Be}$ ,  $^{19}\text{C}$ , and  $^8\text{B}$ . An interesting question is whether a large dipole strength exists near threshold in skin nuclei, or whether it only appears at higher excitation energies, as it usually does in stable nuclei. Since the experimental information about skin nuclei is very limited, it is useful to see what the self-consistent Hartree-Fock and RPA calculations predict.

The low-lying dipole response of halo nuclei is usually calculated as the independent-particle response of the valence nucleon(s) to the dipole operator associated with Coulomb dissociation. In RPA calculations, the basic mechanism which may deplete the low-lying dipole strength is a strong coupling (residual interaction) to the isovector GDR. This coupling is strong if there is a large spatial overlap between the densities of the valence and the core nucleons. Only if the two densities are well separated in space, as they are in halo nuclei, will the low-lying dipole strength

survive in the isovector channel. In stable and in skin nuclei, on the other hand, the spatial separation of the two densities is less dramatic, and the residual interaction will push the threshold strength to higher excitation energies in the isovector channel. This is indeed the result that has been obtained in RPA calculations, for example, for the unstable nuclei  $^{34}\text{Ca}$  and  $^{60}\text{Ca}$ .<sup>2</sup> The experimental implications are that Coulomb dissociation cross sections of skin nuclei will be modest compared to those observed for halo nuclei.

A somewhat surprising feature of the RPA calculations is that a large dipole strength is predicted at lower excitation energies (below 10 MeV) in the isoscalar channel, namely, as a compression mode. This excitation mode can be populated by nuclear interactions with a target nucleus but it remains to be seen how important it is.

The isoscalar quadrupole response of skin nuclei is predicted to be much broader than in stable nuclei, and a substantial strength is predicted below the peak of the isoscalar GQR. The isovector quadrupole strength is spread over a wide range of excitation energies, both in skin and stable nuclei. This work has been accepted for publication.<sup>1</sup>

\*University of Aizu, Japan

<sup>1</sup>H. Sagawa and H. Esbensen, Nucl. Phys. A, in press.

<sup>2</sup>I. Hamamoto, H. Sagawa, and X. Z. Zhang, Phys. Rev. C **57**, 1064 (1998).

### c.6. Many-Body Wave Functions (R. R. Chasman)

We are continuing the development of many-body variational wave functions that put pairing and particle-hole two-body interactions on an equal footing. The variational parameters are calculated with an iteration procedure. The complexity of the wave functions depends only on the number of levels included in the valence space, but does not depend on the number of nucleons in the system. In these wave functions, we conserve particle number and parity strictly, projecting states of good particle number and parity before carrying out the variational calculations. We have added a cranking term to the many-body Hamiltonian and modified the projection procedure to get states of good signature before variation. This allows us to study pairing collapse as a function of angular momentum.

We have also extended the program to calculate spectroscopic factors involved in proton decay. This is useful for studies of nuclides near the proton drip line.

By using residual interaction strengths (*e.g.* the quadrupole interaction strength or pairing interaction strength) as generator coordinates, one gets many different wave functions, each having a different expectation value for the relevant interaction mode. Such wave functions are particularly useful when one is dealing with a situation in which a configuration interaction treatment is needed. This is particularly true for an adequate treatment of pairing at high spin as well as for instances in which the single-particle level density is low. Because the same basis states are used

in the construction of all of the many-body wave functions, it is possible to calculate overlaps and interaction matrix elements for the many-body wave functions obtained from different values of the generator coordinates (which are not in general orthogonal) easily. The valence space can contain a very large number of single-particle basis states, when there are constants of motion that can be used to break the levels up into groups.

Wave functions of this sort become more realistic as the size of each of the groups is increased. To increase this size, we have parallelized our code to run on the SP computer system. We have also modified our codes to handle arbitrary two-body matrix elements. This latter feature allows us to include coulomb matrix elements easily. Together with J.L. Egido and L.M. Robledo, we

have developed subroutines for calculating Gogny interaction matrix elements and coulomb matrix elements for this many-body code.

In the past year, we have made a major speedup in the running times associated with each iteration of a given case by improvements in the parallelization of our code. We found that one of the subroutines could be profitably broken up and distributed among several processors, leading to speedups of a factor of roughly 2.5, for subgroups containing 7 levels, in spite of the increased overhead associated with the additional input and output. We anticipate that the speedups will be even larger for subgroups containing more levels. Increasing the size of the subgroups will allow us to get yet more realistic descriptions of nuclear properties.

### c.7. Very Extended Shapes in Nuclei (R.R. Chasman)

In the past few years, large computer resources have become available on the massively parallel processor IBM SP system at Argonne, in addition to the resources provided by NERSC. We have parallelized the code used to calculate single-particle spectra to exploit the SP system and have devoted a large part of our efforts to calculating energy surface in a four-dimensional shape space that includes reflection asymmetric shapes. We study the nuclear energy surfaces as a function of mass, charge, shape and angular momentum, using the Strutinsky method. In this approach, one makes quantum corrections to a smooth liquid-drop behavior using the calculated single-particle energy levels. In earlier studies, we found that it is often not sufficient to use only quadrupole and hexadecapole deformations to describe very extended reflection-symmetric nuclear shapes. When we added a necking degree of freedom, we found previously unknown minima. These minima are characterized by very extended capsule-shaped nuclei with axis ratios of 2.2:1 in the  $A=180$  mass region. We have now added octupole deformation to this shape space. The inclusion of these two degrees of freedom to our shape space substantially increases our ability to describe nuclear shapes compared to a typical shape space consisting only of quadrupole and hexadecapole deformations. As parity is no longer a good quantum number when octupole deformation is included, the size of the matrices that we diagonalize is doubled. In a typical calculation, we diagonalize matrices that are  $600 \times 600$ . Several thousand such diagonalizations are needed to determine energy surfaces.

There remains a need to test calculated fission barriers and to generally understand nuclear properties at the highest spins. Using the four-dimensional deformation space described above, we have analyzed the high-spin energy surfaces of the  $N=86$  isotones going from Sn ( $Z=50$ ) to Dy ( $Z=66$ ). There is a high-spin superdeformed minimum in all of these nuclides ( $\sim 1.85:1$  axis ratio) that becomes yrast at high spin. These shapes are well known experimentally in the Dy region.

We find that as the proton number decreases from  $Z=66$  to  $Z=50$ , the fission barrier increases by roughly 10 MeV at a given angular momentum. The superdeformed minimum associated with  $N=86$  is present for both Sn and Dy. This result suggests that we can extend the study of nuclear properties at extreme deformations to a new regime of angular momenta, with the availability of radioactive nuclear beam facilities. A preliminary version of this work has been published.<sup>1</sup>

We have extended our high-spin Strutinsky calculations<sup>2</sup> to nuclei in the  $A=100$  mass region. Many of the very extended minima that we find will be accessible with projectiles produced at an exotic beam facility. However, our calculations show very extended minima in nuclides in the vicinity of  $^{108}\text{Cd}$  that are accessible using existing facilities. Recent experiments, inspired by these calculations, show a superdeformed rotational band in  $^{108}\text{Cd}$ .



Several odd-parity excited states have been found in the superdeformed minima of the Hg region. Because of their low excitation energies, it had been thought that these states are very collective. Making use of a particle-number-conserving treatment of pairing, we found<sup>3</sup> that one can calculate the excitation energies of these states quite well as simple broken-pair excitations; using conventional pairing force strengths

and the single-particle levels that were obtained when superdeformation in this mass region was first<sup>4</sup> predicted. The transition matrix elements connecting these excited states to the superdeformed yrast band remain to be explained.

We are analyzing nuclides in the region  $70 < A < 100$ , searching for very extended minima.

<sup>1</sup>R.R. Chasman, Workshop on the Science for an Advanced ISOL Facility, p. 69 (1997)

<sup>2</sup>R.R. Chasman, ANL preprint PHY-9018-TH-98.

<sup>3</sup>R.R. Chasman, Phys. Rev. Lett. **80**, 4610(1998).

<sup>4</sup>R.R. Chasman Phys. Lett. B **219**, 227 (1989).

### c.8. Single-Particle States in the Heaviest Elements (I. Ahmad and R. R. Chasman)

The search for superheavy elements has been a major theme of nuclear structure research for the past twenty years. Theoretical predictions of the stability of superheavy elements depend crucially on the single-particle energy level spacings in the vicinity of 114 protons and 184 neutrons. Our approach is to learn as much as possible about these levels from spectroscopic studies of nuclides in the  $A=250$  region. This is possible because there are members of the relevant spherical multiplets that drop rapidly in energy with increasing deformation, and are fairly close to the ground state in the strongly deformed nuclides near  $A=250$ . The orbitals that are important for fixing the shell corrections near  $N=184$  are the  $h_{11/2}$ ,  $j_{13/2}$  and  $k_{17/2}$  spherical states. For each of these spherical orbitals, there is a corresponding deformed orbital whose energy in the  $A=250$  region is quite sensitive to one of these spherical states, e. g. the  $1/2^-$ [761] orbital that has already been identified in  $^{251}\text{Cf}$  is quite sensitive to the energy of the spherical  $j_{13/2}$  orbital. The position of the  $1/2^+$ [880] deformed orbital is very sensitive to the single particle energy of the  $k_{17/2}$  spherical state. We have calculated signatures for the low-lying states in  $^{251}\text{Cf}$  and the calculated energies and signatures are in good agreement with the experimentally observed (d,p) spectrum. We expect to see the high spin states in a  $(\alpha, ^3\text{He})$  transfer reaction. As a  $^{250}\text{Cf}$  target is not available, we have studied the high spin states in  $^{249}\text{Cm}$ , which is an isotone of  $^{251}\text{Cf}$ . The  $(\alpha, ^3\text{He})$  experiment has been carried out and two high spin peaks have been observed at  $\sim 1.6$  and  $1.9$  MeV. These peaks are candidates for the  $1/2^+$  [880] band. Additional coincidence studies will be needed to make a definitive assignment. This study<sup>1</sup> is published.

Using the Strutinsky method, we found<sup>2</sup> that we could get very good agreement with the known low-lying levels in  $^{251}\text{Cf}$  using a Woods-Saxon potential. We have used the potential parameters generated from this fit to study the stability of superheavy elements. To determine potential parameters for protons in the heavy elements, we utilized data from our spectroscopic studies of  $^{255}\text{Md}$ . These studies show the  $1/2^-$ [521] orbital to lie above the  $7/2^-$ [514] orbital, but the magnitude of the energy difference is not known. Determining the potential in this way, we extrapolate directly to the superheavy element region. As the usual zero-point correction to mass estimates is questionable in that it treats only the quadrupole deformation mode, we replaced this correction in our mass estimates by a term that depends quadratically on the sum of the proton and neutron shell corrections. This correction is easy to evaluate and gives quite reasonable corrections where masses are known. Using the potential parameters derived from the heaviest elements for which there is detailed spectroscopic information, we find that our calculated lifetimes are sufficiently long so as to be able to observe elements at least through  $Z=120$ .

In our analysis, we have assumed that the  $1/2^-$ [521] orbital lies just above the  $7/2^-$ [514] orbital in  $^{255}\text{Md}$ . In fact, this level spacing is not yet known. Our estimates of superheavy element stability will be affected by the experimental value of this level spacing. We hope to determine this spacing through experimental studies, and thereby refine our estimates of superheavy element lifetimes. Another important feature in determining the binding energy of superheavy elements is the magnitude of the pairing interaction strength.

We have recently completed a study<sup>3</sup> of excited states in  $^{256}\text{Fm}$ , which is the heaviest nucleus in which excited non-rotational states have been observed. We have used the  $I=7$  negative parity state at 1426 KeV in this nuclide to adjust the proton-pairing interaction strength. Our calculated spectrum for other proton broken-pair states is in good agreement with those that have been observed, and we predict many other such states between 1 and 2 MeV. Pinning down the proton-pairing strength, in the heaviest nuclide where there is sufficient data to do so, improves the reliability of predictions of the stability and structure of yet heavier elements.

Additionally, we have studied<sup>3</sup> the decay of  $^{255}\text{Md}$  to determine low-lying single-particle state assignments in  $^{255}\text{Fm}$  and  $^{251}\text{Es}$ . Through studies such as these, we hope to get an accurate picture of nuclear structure on both sides of the deformed neutron single-particle gap at  $N=152$  and the deformed proton gap at  $Z=100$ .

We have completed an analysis<sup>4</sup> of excited states in  $^{251}\text{Cf}$  populated in the alpha decay of  $^{255}\text{Fm}$ . This allowed us to characterize several single-particle and vibrational states beyond the  $N=162$  deformed gap.

<sup>1</sup>I. Ahmad *et al.*, Nucl. Phys. **646**, 175 (1999).

<sup>2</sup>R. R. Chasman and I. Ahmad, Phys. Lett. B **392**, 255 (1997).

<sup>3</sup>I. Ahmad, R.R. Chasman and P.R. Fields Phys. Rev. C **61**, 044301 (2000)

<sup>4</sup>I. Ahmad *et al.*, Phys. Rev. C **62**, 064302 (2000).

### c.9. Studies of Nuclear Energy Surfaces (R.R. Chasman , J. L. Egido and L.M. Robledo)

This collaborative research program is focused on the study of nuclear energy surfaces, with an emphasis on very deformed shapes using several complementary methods: 1) the Strutinsky method, 2) Hartree-Fock-Bogoliubov calculations using the Gogny interaction, and 3) many-body variational wave functions that we have described above.<sup>1,2,3</sup> Our strategy is to identify phenomena and nuclides of interest using the Strutinsky method and to study the most interesting cases with the HFB and many-body approaches. The latter approaches include many-body effects and describe these features more accurately.

The great advantage of the Strutinsky method is that one can study the energy surfaces of many nuclides ( $\sim 300$ ) with a single set of calculations. Although the HFB and many-body (MB) calculations are quite time consuming relative to the Strutinsky calculations, they have many advantages. For the studies of the Pb isotopes described below, they have the advantage that configuration interaction effects can be easily incorporated into the calculations. In this way, we deal directly with the issue of insuring the orthogonality of states that have the same spins and parities.

The neutron deficient nuclides ( $N < 110$ ) in the Pb region have states that are characterized by three distinct shapes: spherical, prolate and oblate. In the oblate and prolate minima, there are low-lying single-particle states derived from spherical states on both

sides of the  $Z=82$  single-particle gap. Although this gap is roughly 4 MeV, there are states within a few hundred keV of ground in the neutron deficient Tl( $Z=81$ ) and Bi( $Z=83$ ) isotopes that would be at  $\sim 4$  MeV excitation, in the simplest single-particle picture. Our approach is to determine the nuclear wave function as a function of quadrupole moment, letting other deformation modes (*e.g.* P4 and P6) vary freely. Using both the HFB and MB methods, we find three low-lying state in the results. In both the HFB and MB calculations, the three separate low-energy  $0^+$  states persist after the configuration interaction is taken into account. These are the first calculations that give a  $0^+$  oblate state in  $^{186}\text{Pb}$ , in agreement with the experimental observation of two  $0^+$  excited states in this nuclide. In Fig. V-11, we show the results obtained with the Gogny interaction. Both calculations also predict an as yet unobserved  $0^+$  state in  $^{184}\text{Pb}$ . Investigations are under way to search for this state.

Proton emission has been observed<sup>4</sup> in the light Pb nuclei. It seems that one might hope to use this phenomenon to extract some interesting spectroscopic data on nuclear shapes and orbitals in much the same way that one gets spectroscopic information through single-nucleon transfer reactions such as (d,p) and (d,t) reactions. In order to explore this possibility, we have developed a treatment of proton-emission spectroscopic factors using the MB wave functions. In the case that we have studied ( $^{185}\text{Bi} \rightarrow ^{184}\text{Pb}$ ), the energetics of the

reaction are such that only the ground state is populated. We calculate a very small spectroscopic factor for the proton decay to the ground state. The small spectroscopic factor is largely due to the shape difference between the deformed decaying state in  $^{185}\text{Bi}$

and the ground state of  $^{184}\text{Pb}$ , which is spherical. To understand this spectroscopic factor, it is necessary to have good wave functions for the initial and final states. A systematic study of this region should provide us with improved wave functions.

\*Universidad Autonoma de Madrid

<sup>1</sup>R. R. Chasman and L. M. Robledo, Phys. Lett. B **351**,18 (1995).

<sup>2</sup>J. L. Egido, L. M. Robledo, and R. R. Chasman, Phys. Lett. B **393**, 13 (1997).

<sup>3</sup>L. M. Robledo, J. L. Egido, and R. R. Chasman Proceedings of the Conference on Nuclear Structure at the Limits, July 22-26,1996, p. 124.

<sup>4</sup>C. N. Davids *et al.*, Phys. Rev. Lett. **76**, 592 (1996).

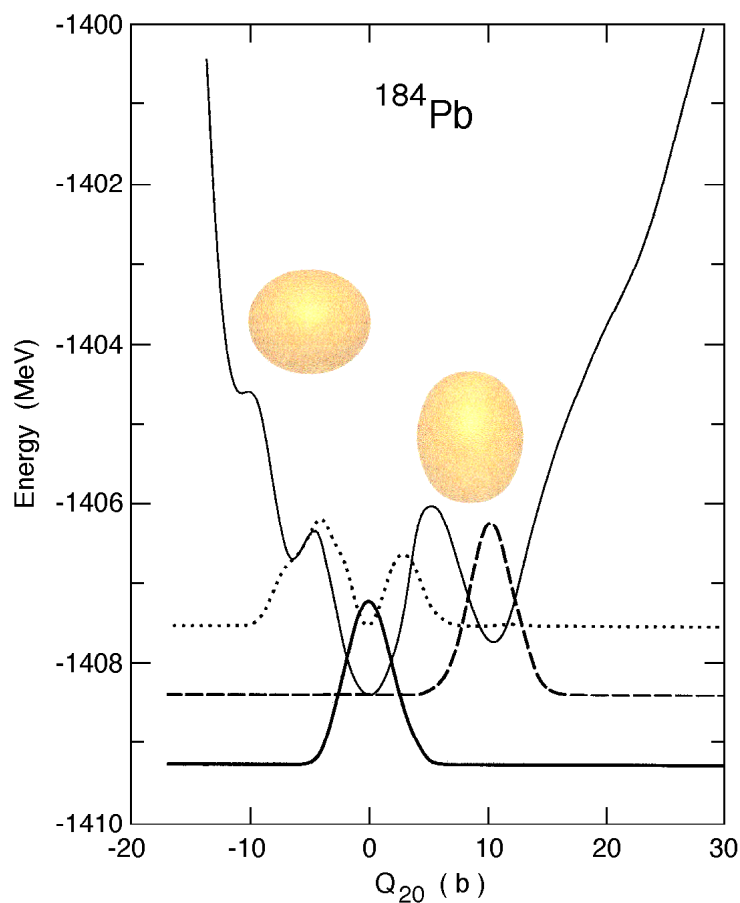


Fig. V-11. The thin solid line shows the energy calculated as a function of quadrupole moment. There are three distinct minima. The dotted, dashed and thick solid lines show the distribution of the three low-lying  $0^+$  states as a function of quadrupole moment after the configuration mixing calculation is done. The differences of the flat parts of the latter curves, at large quadrupole moments, give the calculated energies.

### c.10. Neutron-Proton Pairing (R. R. Chasman)

In most nuclides, the fermi levels of protons and neutrons are sufficiently different that  $T=1$  n-n and p-p pairing are the dominant particle-particle residual interaction modes. In nuclides with roughly equal numbers of protons and neutrons, one expects that the  $T=1$  n-p interaction will also play an important role, as well as the  $T=0$  n-p interaction. In order to get a good handle on these effects, it will be necessary to go beyond the quasi-particle approximation. To get a clear

signal of n-p pairing, it is necessary to study not only nuclei along the  $N=Z$  line, but also the nuclides in the vicinity of the  $N=Z$  line. This cannot be done in the usual n-p quasiparticle formalism. We are in the process of extending our many-body approach to include n-p interactions. With the advent of a rare isotope accelerator, we anticipate that considerable spectroscopic information will become available on nuclides near the  $N=Z$  line.

## D. ATOMIC THEORY AND FUNDAMENTAL QUANTUM MECHANICS

In addition to research on hadronic and nuclear physics, we also conduct research in atomic physics, neutron physics, and in areas related to quantum computing.

Recent work in atomic physics includes the studies of the interactions of high-energy photons with matter, in support of experiments performed at Argonne's Advanced Photon Source (APS). Theoretical studies are being conducted on the physics of Compton scattering by bound electrons, focusing on topics selected in view of basic importance, timeliness, and potential in applications. We also produced a review on "Electron collision cross sections of atoms" for inclusion in a forthcoming volume on "Atomic Collisions" in the Landolt-Boernstein Numerical Data and Functional Relationships series.

Our studies in neutron physics include basic issues in the design and interpretation of neutron interferometry experiments and providing theoretical support for the design of a new experiment to measure the neutron's electric-dipole moment. The status of that experiment is reported in item f.3 of the Heavy-Ion Section of this report.

Our work on areas related to quantum computing has focused on two areas: the use of quantum robots to search space regions, and the mathematical and physical assumptions involved in representing the nonnegative integers by quantum states of physical systems. The combination of quantum robots to locate a system with Grover's algorithm to process the search results was examined to see if the quantum search was more efficient than a classical robot search. It is seen that quantum searches in regions of three or more dimensions are more efficient than classical searches with the efficiency increasing with the number of dimensions.

Studies of the representation of natural numbers by quantum states of physical quantum systems were based on modeling the axioms of number theory or arithmetic by states of quantum systems. An abstract model of the axioms as states in and operators on a tensor product of Hilbert spaces served as a common reference for models of physical systems. The sensitivity of different quantum algorithms to details of maps from the abstract to the physical models was described. Also the important requirement of efficient physical implementability of the arithmetic operations described by the axioms, as a restriction on acceptable physical models, was investigated.

### d.1. Interactions of Photons With Matter (M. Inokuti and D. Y. Smith)

In support of experiments in atomic and condensed-matter physics with the use of synchrotron radiation, theoretical studies are being conducted on the physics of photo-absorption and Compton scattering, focusing on topics selected in view of basic importance, timeliness, and potential applications.

One theme of long-term studies has been the use of dispersion relations and sum rules for indices of responses of matter over the entire range of photon

energies. A comprehensive analysis of optical data on silicon<sup>1</sup> is in progress, and a new expression for the refractive index in a region of near transparency<sup>2</sup> is applied to graphite, silicon, and germanium.

A sum rule for the absorption strength originally due to Vinti<sup>3</sup> is applied to color centers in alkali halides to derive the spatial extent of the electronic structure of the color centers.<sup>4</sup>

---

<sup>1</sup>D. Y. Smith, M. Inokuti, and W. Karsten, *Physics Essays*, in press.

<sup>2</sup>D. Y. Smith and M. Inokuti, submitted to *J. Phys. C: Condensed Matter*.

<sup>3</sup>J. P. Vinti, *Phys. Rev.* **41**, 432 (1932).

<sup>4</sup>D. Y. Smith and M. Inokuti, submitted to *Radiat. Effects Defects Solids*.

### d.2. Interactions of Charged Particles With Matter (M. Inokuti)

Stopping power, the total yield of ionization, and its statistical fluctuations are examples of quantities describing the penetration of charged particles through matter, and are important to applications such as the detection of particles and the analysis of their charges and kinetic energies. The understanding of those quantities in terms of individual collisions and associated cross sections remains a major challenge, and is the goal of our continuing effort. Recent activities include the following: A comprehensive set of

cross sections of liquid water for interactions of energetic protons has been determined<sup>1</sup> through critical evaluation of pertinent data. A review<sup>2</sup> of cross sections for electron collision with atoms has been published. Unpublished materials left by R. L. Platzman (1918-73) a pioneer of radiation physics and chemistry and a former Argonne staff member (1958-65) have been studied,<sup>3</sup> and prepared for an archive in the Joseph Regenstein Library of the University of Chicago.

---

<sup>1</sup>M. Dingfelder, M. Inokuti, and H. G. Paretzke, *Radiat. Phys. Chem.* **50**, 255 (2000).

<sup>2</sup>M. Inokuti, in *Landolt-Börnstein Numerical Data and Functional Relationships in Science and Technology*, ed. Y. Itikawa (Springer-Verlag, Berlin 2000) Vol. 1/17, p. 2-1.

<sup>3</sup>M. Inokuti, *Radiat. Phys. Chem.*, in press.

### d.3. Superluminal Behavior in Wave Propagation (M. Peshkin)

Recently published claims to have observed superluminal behavior of microwaves have attracted significant attention. The authors created a Bessel beam of the form

$$A = A_0 J_0(\rho k \sin \theta) \exp\{I(zk \cos \theta)\},$$

where  $\theta$  is a fixed angle around  $20^\circ$ . They found experimentally that chopped segments of that beam progressed along the  $z$  axis at the superluminal speed  $v=c/\cos\theta$  and they presented theoretical calculations to show that their experimental result agrees with the group velocity of such a wave packet. They made no claim of having violated Einstein causality.

I have shown that a correct calculation of the group velocity actually yields the subluminal value  $v=c \cos\theta$ , contrary to the experiment. In fact if the experiment is correct then Maxwell's equations are grossly in error at microwave frequencies.

It is not obvious from the published report how the experimental result could be wrong. One possibility is that the Bessel wave was actually not perfectly symmetric around the  $z$  axis but contained an enhanced plane wave component propagating at an angle  $\theta$  to the  $z$  axis in the neighborhood of some azimuth. Such a plane wave would travel with the usual light speed  $c$  but would reach successive detectors placed along the  $z$  axis at time intervals that would give the illusion of waves moving in the  $z$  direction with speed  $c/\cos\theta$ . This work was posted on the Los Alamos archive.<sup>1</sup>

<sup>1</sup>M. Peshkin, Los Alamos Archives preprint, physics/0006034.

### d.4. Space Searches with a Quantum Robot (Paul Benioff)

Work was completed on the description of quantum robots used to search a volume of space to determine the unknown position of a system. A quantum robot is a mobile quantum system that includes an on-board quantum computer and ancillary memory, output, and control systems. The motivation was to see if one could combine a quantum description of the search process with the efficiency gain of Grover's algorithm<sup>1</sup> to show that such a quantum search is more efficient than any classical search process. Grover's algorithm is a quantum search algorithm of a completely unstructured data base of  $m$  elements that carries out

the search for a single element in  $O(m^{1/2})$  steps ( $O(-)$  means "of the order of") compared to  $O(m)$  steps in a classical search procedure.

It was found that a search of a  $d$ -dimensional space lattice cube with  $N^d$  sites for a system located at one of the sites requires  $O(N^{1+d/2} \log N)$  steps compared to  $O(N^d \log N)$  steps for a classical search.<sup>2</sup> This shows that a quantum search is more efficient than a classical search for  $d > 2$ . For three-dimensional space searches the quantum search is only marginally better than a classical search.

<sup>1</sup>L. K. Grover, in Proceedings of 28th Annual ACM Symposium on Theory of Computing (ACM Press New York 1996), p. 212; Phys. Rev. Lett. **79**, 325 (1997); G. Brassard, Science **275**, 627 (1997).

<sup>2</sup>P. Benioff, Space Searches with a Quantum Robot, to appear in Proceedings, AMS Special Session on Quantum Computing, AMS annual meeting, January, 2000.

### d.5. The Representation of Numbers in Quantum Mechanics (Paul Benioff)

Work was continued and completed for publication<sup>1</sup> on the mathematical and physical assumptions and conditions involved in the representation of the nonnegative integers or natural numbers by states of physical systems. The view taken is that any nonempty set is a set of natural numbers if it satisfies (or is a model of) the axioms of number theory or arithmetic. This applies to sets of both mathematical and physical systems. The work was limited to k-ary representations of length L. A model of the axioms based on number representation states of the form  $|s\rangle = \bigotimes_{j=1}^L s(j)$  in an L fold tensor product space H of k-dimensional Hilbert spaces of states was described. Here s is a function from L to the numbers 0,1,...,k-1. Definitions of addition and multiplication operators were given based on definitions of successor operators  $V_j$  for each  $j=1,2,\dots,L$ . The  $V_j$  correspond to addition of  $k^{j-1}$ . These operators were shown to satisfy the axioms of number theory modified for the presence of L different successor operations.

Unitary maps of  $H^{\text{arith}}$  to other Hilbert spaces  $H^{\text{phys}}$  of states of composite physical systems were described. These maps induce representations of the  $V_j$ , addition, and multiplication operators on the physical space of states. Grover's algorithm and Shor's algorithms are

shown to be quite different regarding their sensitivity to details of the unitary maps.

The main physical condition that must be satisfied is that the basic arithmetic operations must be efficiently implementable. This condition means that for each basic arithmetic operation there must exist a corresponding Hamiltonian associated with physical implementation of the operation on the physical states of the quantum system. In addition there must exist a physical procedure for carrying out or implementing each Hamiltonian, and the space-time and thermodynamic resources needed for implementation must be at most polynomial in L. The resources required cannot be exponential in L.

This is the main restrictive condition that excludes many physical systems as models for the natural numbers. It is also the reason for defining the  $V_j$  separately for each j and requiring that each be efficiently implementable. Without this condition, there is no guarantee that the  $V_j$  are efficiently implementable even if the simplest successor operator  $V_1$  were efficiently implementable. This follows from the basic relation  $V_{j+1} = (V_j)^k$  for k-ary representations.

<sup>1</sup>Paul Benioff, Phys. Rev. A **63**, 032305 (2001).

## E. OTHER ACTIVITIES

### e.1. Perspectives in Continuum Strong QCD (M. B. Hecht, C. D. Roberts, and S. M. Schmidt)

We organized a Theory Institute over the five days: 14-18 August 2000, which canvassed a range of topics in contemporary strong interaction physics: Hadron Spectroscopy and Exotics; Light-Hadron Form Factors and Sum Rules; Heavy-Quark Observables; and Quark-Gluon Plasma -- Theory and Phenomenology. These areas are distinguished by the fact that continuing progress requires the development and application of

models and continuum nonperturbative techniques. Attendance was deliberately limited to thirty participants in order to encourage a true workshop atmosphere. The Institute achieved its aim of fostering discussions between experts in those intuition-building, nonperturbative theoretical tools that are crucial for the anticipation and interpretation of the current generation of hadronic physics data.

**e.2. 13th Annual Midwest Nuclear Theory Get-Together (R. B. Wiringa)**

The Theory Group hosted the Twelfth Annual Midwest Nuclear Theory Get-Together on September 22 and 23, 2000. Nuclear theorists from a number of midwest universities get together every fall to find out what different people and groups in the region are working on. The organizational duties rotate among the participants, but Argonne has become the regular meeting place by virtue of its facilities and central location. The organizer for 2000 was Richard Furnstahl of Ohio State University. The meeting provides a good chance for students to broaden their horizons and get some practical speaking experience in a friendly atmosphere. The format is very informal, with an

agenda of talks being volunteered at the beginning of the meeting. This year we tied for the largest attendance ever: 30 faculty, postdocs, and students from eleven different universities in Illinois, Iowa, Kansas, Kentucky, Michigan, Minnesota, Missouri, Ohio, and Wisconsin, along with the Argonne staff. Some 24 presentations were made over Friday afternoon and Saturday morning. Topics included relativistic quantum mechanics, gauge and effective field theories, QCD, quantum Monte Carlo methods, nuclear pairing, no-core shell model, relativistic heavy-ion collisions, and neutron matter. A good time was had by all.